EVOLUTION OF A TURBIDITE SYSTEM IN A NARROW BASIN SETTING: THE ROPIANKA FM (CAMPANIAN–PALEOCENE) IN THE SKOLE NAPPE OF THE POLISH CARPATHIANS

Piotr ŁAPCIK

Jagiellonian University, Faculty of Geography and Geology, Institute of Geological Sciences,
Gronostajowa 3a, PL-30-387 Kraków, Poland; e-mail: piotr.lapcik@.uj.edu.pl

Abstract: The deposits of the Turonian–Paleocene Ropianka Fm (Skole Nappe, Polish Outer Carpathians) were subdivided into 11 sedimentary facies and subsequently 7 facies associations, corresponding to different depositional environments of the turbidite system. The depositional setting includes a wide range of processes in sedimentary environments from proximal channel-fill deposits to channel-lobe transition zone and a full spectrum of lobe sub-environments, i.e., lobe-axis, off-axis and lobe-fringe, distal-fringe, and interlobe areas. The Campanian–Paleocene evolution of the western Skole Basin shows several progradational-retrogradational cycles and corresponding shifts from carbonate- to siliciclastic-dominated sedimentation, mostly as a result of relative sea-level changes and tectonic activity. The progradational-retrogradational cycles start with the appearance of sand-rich bodies, which tend not to occur up the succession. Four evolutionary stages are distinguished, including 1) the early Campanian marlstone-dominated sedimentation (Kropivnik Fucoid Marl Mbr) in the lower-slope or base-of-slope settings, which correlates with a relative sea-level highstand, 2) the late Campanian progradation of the turbidite system with siliciclastic sedimentation (Turnica Flysch Mbr) and a major sediment distribution path, extending along the northern margin of the basin, 3) the Maastrichtian progradational-retrogradational cycle with the influence of a carbonate source, and 4) mixed carbonate-siliciclastic sedimentation (Leszczyny Mbr) with exotic-bearing mass transport deposits (Makówka Slump Debrites and Babica Clay) and a general trend of cessation of carbonate sedimentation up the sections. The complex facies distribution through the time interval studied is the effect of basin asymmetry with a relatively steep southern slope and a gentler northern slope and the action of multiple sediment sources. The highly aggradational trend of particular depositional elements, variability in calcareous sediment content and palaeotransport directions indicate the presence of morphological obstacles and/or the semi-confined character of the western part of the basin.

Key words: Mixed siliciclastic-carbonate sedimentation, quantitative analysis, facies analysis, semi-confined basin.

INTRODUCTION

Facies analysis plays an important role in basin analysis and serves as a tool to track the evolution of fossil depositional environments. This also applies to the deep-water setting, where turbidite systems represent an ultimate sink for the vast majority of sedimentary materials on Earth, including anthropogenic pollutants (e.g., Martin *et al.*, 2022). The consequence of the capturing and burial of these deposits has also a great influence on carbon sequestration and climate (e.g., Arthur *et al.*, 1988). Our understanding of the architecture and evolution of deep-water systems is constantly growing and models for facies prediction are

now better than ever. However, the multiplicity of factors, which strongly influence turbidite systems (e.g., nature of the source, tectonic setting, eustatic sea-level changes, climate), leads to a wide variety of ancient records and proposed models that describe them (e.g., Mutti and Normark, 1987; Mutti, 1992; Reading and Richards, 1994; Pickering *et al.*, 1995; Bouma, 2000; Mutti *et al.*, 2009; Pickering and Hiscott, 2015; Tinterri *et al.*, 2020). Without a quantitative approach, it is very difficult or impossible to compare two different turbidite systems and to analyse the impact of different factors on sedimentation. Hence, collecting

comparable quantitative data and analysis using statistical methods is important for the better description and understanding of depositional systems worldwide.

Previous detailed sedimentological and facies analyses were limited to a few relatively small areas in the central segment of the Skole Nappe and presented the Ropianka Fm as a mixed sand-mud depositional system with well-developed channel-lobe complexes (Łapcik, 2017, 2018, 2019). During the present study, a larger area was investigated in the western part of the Skole Nappe to obtain a larger amount of data and to compare the uniformity of Late Cretaceous–Paleocene sedimentation between the western and central parts of the Skole Basin. The main purposes of this paper are: 1) to descriptively and statistically characterise the deposits of the Ropianka Fm in the western part of the Skole Nappe south of Tarnów and to distinguish the morphodynamic architectural elements of the deep-marine system, 2) to investigate the evolution of the turbidite system in a narrow basin setting, and 3) to give an extended sedimentary background to the Ropianka Fm for future studies.

GEOLOGICAL SETTING

Skole Nappe

The study area is located south of Tarnów, between the Dunajec and Biała rivers, in the western part of the Skole Nappe, which is the most external major lithostratigraphic unit of the Polish Outer Carpathians (Fig. 1). The deposits of the Polish Outer Carpathians are interpreted as the sedimentary infill of several deep marine basins that existed during late Jurassic–early Miocene times in the NE branch of the Tethys Ocean (e.g., Gągała et al., 2012; van Hinsbergen et al., 2020). The sedimentary infill of the Carpathian basins was folded and thrust as a series of imbricated nappes onto the Carpathian Foredeep in the Early and Middle Miocene (Golonka et al., 2006; Ślączka et al., 2012). The margin of the Carpathian thrust and allochthonous folded Miocene deposits bounds the study area to the N. To the S, folded and imbricated thrust sheets of the Silesian and Subsilesian Nappes are thrust onto the Skole Nappe (Fig. 1).

The Skole Nappe contains 3–3.8 km thick sedimentary succession (Oszczypko, 2006), which records post-rift deepening of the Skole Basin (Malata and Poprawa, 2006), through a well-developed turbidite system, to a remnant foreland basin, which was ultimately folded and thrust to the N and NE onto the Carpathian Foredeep during the early Miocene (Kotlarczyk, 1988a; Gągała et al., 2012). During the Hauterivian–Cenomanian the Skole Basin was part of the Severin-Moldavidic Basin, which included sediments deposited at the early stage of the subsequent Silesian, Subsilesian, and Skole Basins (Golonka et al., 2008; Ślączka et al., 2012). The sedimentary succession of the Skole Nappe (Fig. 2) starts with a thin series of Hauterivian calcareous clayey and silty mudstone (~13 m thick, Bełwin Mudstone) and noncalcareous sediments of the Hauterivian–Cenomanian, dominated by black clayey and silty mudstone with a minor contribution of sandstone and siltstone (~220–240 m thick, Spas Shale; Gucik 1963; Kotlarczyk, 1988a; Bąk et al., 2014). The aforementioned deposits are thought

to be related to post-rift thermal subsidence (Malata and Poprawa, 2006). During the Cenomanian–Turonian sedimentation was dominated by black and variegated clayey and silty mudstone (~40 m thick Barnasiówka Radiolarian Shale Fm), formed below the local carbonate compensation depth (Gucik 1963; Bąk et al., 2014). Turonian–Paleogene sedimentation (~1.6 km thick, Ropianka Fm) represents the beginning of the compression stage of the Skole Basin, after its separation from the Severin-Moldavidic Basin with the uplift of the Subsilesian Ridge (Węglówka Ridge) during the Turonian (Golonka et al., 2008). The Ropianka Fm is dominated by deposits of interbedded mudstone, sandstone and conglomerate, with a high contribution of marlstone, mostly in the marginal part of the Skole Nappe (Kotlarczyk, 1978, 1988a). According to Barwicz-Piskorz and Rajchel (2012), the Ropianka Fm is overlain by Paleocene–Eocene red clayey and muddy shales interbedded with green shales and lenses of sandstones (Variegated Shale Fm) up to ~190 m thick and by the Eocene–Lower Oligocene succession, up to ~180 m thick and dominated by green sandstones interbedded with green mudstones (Hieroglyphic Fm). This change in sedimentation marks a deepening of the Skole Basin and a reduction of the sediment supply. The Oligocene Menilite Fm is mostly dominated by noncalcareous, brown, and black mudstone with intercalations of chert, marlstone, diatomite, thick-bedded sandstone, and conglomerate. This sedimentary succession is interpreted as a poorly oxygenated, deep-marine system with elongated fans and the mass redeposition of large olistostromes (e.g., Kotlarczyk et al., 2006). The youngest deposits of the Skole Nappe are represented by ash-grey, typically calcareous mudstones and muscovitic sandstones of the Krosno Fm (Krosno Beds, Kotlarczyk et al., 2006). The boundary between the Menilite Fm and the overlying Krosno Fm is frequently transitional, which often results in the identification of their succession as the Menilite-Krosno Series, reaching ~2.2 km in total thickness (Kotlarczyk et al., 2006).

Stratigraphy of the Ropianka Fm

The Ropianka Fm (after Kotlarczyk, 1978), known as Ropianka Beds (after Paul, 1876), Inoceramian Beds (after Uhlig, 1888) or Rybotycze Fm (after Malata, 1996), consists of calcareous to noncalcareous deposits of various sediment gravity flows with subordinate hemipelagic to pelagic deposits, which may reach up to ~1.6 km thick. The Ropianka Fm is subdivided into 4 members (Fig. 2): the Cisowa Mbr, ~650 m thick (Turonian–lower Campanian), the Wiar Mbr, ~700 m thick (lower Campanian–lower Maastrichtian), the Leszczyny Mbr, ~330–390 m thick (lower Maastrichtian–lower Paleocene) and the Wola Korzeniecka Mbr, ~50 m thick (Paleocene), which show various styles of lateral development and thicknesses (Kotlarczyk, 1978, 1988a, b). Several distinctive layers and intervals of variegated clayey mudstones are distinguished with the rank of the chronohorizons (Kotlarczyk, 1978). However, a more recent lithostratigraphic scheme includes up to 11 members (Malata, 1996).

The Ropianka Fm displays a complex internal architecture, typical of a turbidite system (e.g., Kotlarczyk, 1978,
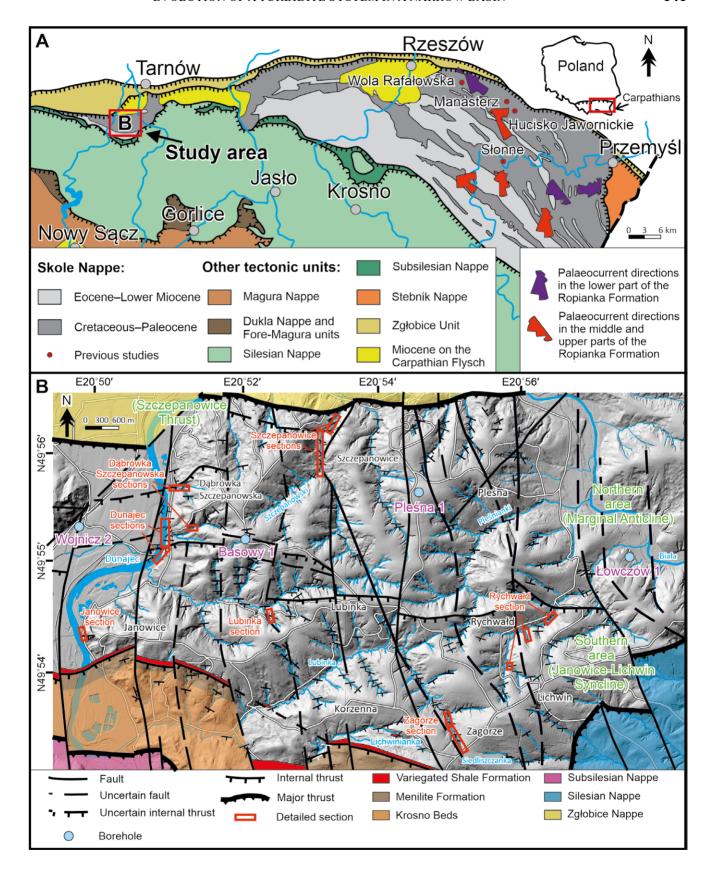
Fig. 1. Location maps of the study area. **A.** Geological map of the eastern part of the Polish Outer Carpathians (based on Cieszkowski *et al.*, 2017 and Żytko *et al.*, 1989, modified), with palaeocurrent directions after Bromowicz (1974). **B.** Study area with an overlay of a hillshade terrain model (https://baza.pgi.gov.pl/cbdg/geoportal). Geology and tectonics are based on Marciniec *et al.* (2006, 2014), with modifications.

1988a, b; Łapcik *et al.*, 2016; Łapcik, 2017, 2018, 2019), which represents a mixed sand-mud system. However, the marginal part of the Ropianka Fm, corresponding to the base-of-slope, or the slope itself, contains a high proportion of marly deposits, which may fully dominate the sedimentary succession, e.g., in the eastern part of the Skole Nappe (Burzewski, 1966; Kotlarczyk, 1978, 1988a; Geroch *et al.*, 1979; Leszczyński *et al.*, 1995; Leszczyński, 2003, 2004; Kędzierski and Leszczyński, 2013). These calcareous deposits form wedges, up to ~170–180 m thick, which occur at the bottom of the Cisowa and Wiar members (Fig. 2) and are diluted by or replaced with siliciclastic-dominated deposits throughout the section (Bromowicz, 1974; Kotlarczyk, 1978). More recently, marlstone-rich sedimentary successions within the Wiar Mbr were reported from a more internal part of the basin (Waśkowska *et al.*, 2019). The Leszczyny Mbr also includes marlstone lenticular

bodies that are randomly distributed in predominantly siliciclastic deposits (Burzewski, 1966; Kotlarczyk, 1978). The youngest Wola Korzeniecka Mbr represents noncalcareous sedimentation and is rarely reported in the Skole Nappe (Kotlarczyk, 1978). Data on palaeotransport within the Skole Basin indicate the predominance of directions towards the SW, S, and SE (Fig. 1A; Książkiewicz, 1962; Bromowicz, 1974).

Study area

The study area is located in the northwestern marginal part of the Skole Nappe and covers an area between the Dunajec and Biała rivers (Fig. 1). The sedimentary succession of the Ropianka Fm was investigated in numerous small to medium outcrops, including an area near the villages and hamlets of Dąbrówka Szczepanowska, Szczepanowice, Janowice, Lubinka, Pleśna, Rychwałd, Zagórze, Korzenna and Lichwin, with additional field observations in the surrounding area. The outcrops are located primarily on the banks of rivers and streams and in natural escarpments. In the study area, palaeotransport directions to the S, SW, NW and N (Koszarski, 1961) are more diverse than the general SE and S trends in the eastern part of the basin (Książkiewicz, 1962; Bromowicz, 1974).

The Skole Nappe in the study area is strongly affected by tectonic deformation and consists of internally deformed, imbricated thrust sheets, i.e., 1) the complex Marginal Anticline to the north, which is thrust onto the internally deformed Zgłobice Nappe and 2) the Janowice-Lichwin Syncline, which passes into an anticline, thrust onto the Ropianka Fm deposits in the southern part of the study area (Marciniec *et al.*, 2014). On the basis of micropalaentological data and surface tectonic deformation, an additional small thrust (Szczepanowice Thrust) was marked in the northernmost part of the area (Fig. 1B). In general, the deposits of the Ropianka Fm dip the S and SE, more rarely to the E (Fig. 1B).

METHODOLOGY

Most of this study is based on standard sedimentological fieldwork with high-resolution bed-by-bed logging of the stratigraphic succession and classification of sedimentary facies as a record of specific depositional processes. During the investigation of outcrops, special attention was paid to lithology, bed thickness, textural properties, primary depositional and erosional structures, lower and upper bedding surfaces and deformational structures, with additional documentation with digital photography. Measurements of the size and orientation of sedimentary structures were integrated with the logging, using a standard geological compass (233 measurements). More than half of the palaeocurrent measurements were collected from ripple and dune cross-lamination, which is more susceptible to flow deflection and/or reflection than sole marks.

A series of samples was collected for further sedimentological and facies analysis, including analysis on cut surfaces (57 samples). Thirty poorly lithified sandstone samples were collected from the Janowice section at
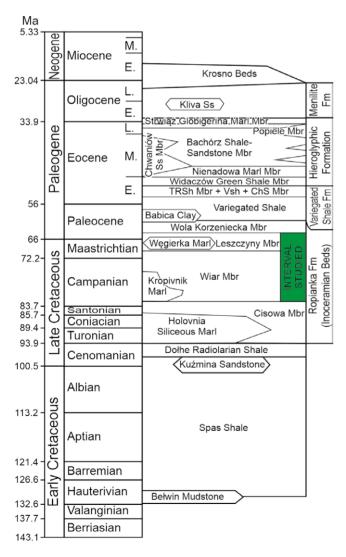

Fig. 2. Stratigraphic scheme of the Skole Nappe, based on Kotlarczyk (1988a), Rajchel (1990), Rajchel and Uchman (1998) and Ślączka and Kaminski (1998), with modifications by Gedl (1999), Kotlarczyk *et al.* (2006) and Gasiński and Uchman (2009). The time scale is according to Gradstein *et al.* (2020). Abbreviations: TRSh Mbr – Trójca Red Shale Mbr; VSh – Variegated Shale; and ChS Mbr – Chmielnik Stripy Sandstone Mbr.

10–20 cm intervals for analysis of the grain sizes of massive thick-bedded sandstones with the laser diffraction method, using Mastersizer 3000. Samples for grain size analysis were dried in an oven at 80–100°C for 8–10 h. The samples were then weighted, gently disintegrated mechanically and quartered. The grain-size analysis was carried out using a wet hydro dispersion unit and its results are summarised in Supplementary Material 1, Table S1.

The logged deposits were described and classified as sedimentary facies, linked to distinctive depositional processes. Most of the facies identified in this study show similarities with the facies described in other deep-water depositional systems (e.g., Pickering and Hiscott, 2015; Tinterri *et al.*, 2020). Further vertical and spatial analysis of the sedimentary logs allowed the recognition of assemblages of related sedimentary facies (facies associations), which were interpreted as representatives of well-established architectural elements (depositional sub-environments) of the deep-water sedimentary system (e.g., Mulder, 2011; Pickering and Hiscott, 2015). For an unbiased interpretation, a statistical representation of facies and facies associations was prepared.

Samples of marlstone and mudstone were collected for micropalaeontological analysis of biostratigraphic age, using foraminifers and calcareous nannoplankton to facilitate stratigraphic interpretation and correlation between the studied logs. The 'Short spin' technique (vide Edwards, 1963; Perch-Nielsen, 1985) was used for calcareous nannoplankton samples, which were analysed under a Nikon Eclipse E600 Pol cross-polarised light microscope at 1000x magnification. Calcareous nannoplankton assemblages were distinguished using Calcareous Nannofossil Biostratigraphy (Bown and Young, 1998) and the website Nannotax3 (http://www.mikrotax.org/Nannotax3/). The biostratigraphic age was determined using Boreal (BP) and Tethys (TP) biozonation (Burnett, 1998), owing to the cooccurrence of taxa from both provinces. Samples for the micropalaeontological analysis of foraminifers were disintegrated following standard micropalaeontological procedures with Glauber salt or liquid nitrogen. The samples were then washed in 1000, 500 and 63 μm sieves and after drying, at least 300 isolated foraminifera specimens were collected from the >125 μm fraction. Then the foraminifer assemblages were quantitatively analysed. For species designations, the Prolab MSZ 2005 stereomicroscope was used. The results of the micropalaeontological analysis are summarised in Supplementary Material 2, Table S2.

On the basis of the local tectonic setting, the study area was subdivided into the northern and southern areas, according to the line of thrust (cf. Marciniec *et al.*, 2006, 2014). Stratigraphic correlation between the sections studied is the result of analysis and comparison, based on several independent sets of data. First, visited and logged sections were categorised on the basis of their characteristic facies composition and similar order of facies associations distinguished. The most characteristic facies associations include marlstone-dominated sections and sections with a large amount of thick-bedded sandstone. Secondly, the spatial continuity of the characteristic sand-rich intervals allowed the recognition of four sandy bodies (SB1–4), which were correlated using the strike and dip of beds, the digital elevation model (airborne laser scanning image of land surface LiDAR available

on the website of the Polish Geological Institute National Research Institute (https://baza.pgi.gov.pl/cbdg/geoportal), and previous covered and uncovered geological maps with explanations (Marciniec *et al.*, 2006, 2014). In some sections, auxiliary dating of the collected micropalaeontological samples was conducted. The final result was compared with well log data (stratigraphy and lithology) from the boreholes Wojnicz 2, Basowy 1, Pleśna 1 and Łowczów 1 marked in the Figure 1B and the wells Pleśna 2, Tarnów 14, Łowczów 2, Grabek 1, Grabek 2, and Olszyny 1 in the close vicinity of the study area. All well log data considered are available on the website of the Polish Geological Institute National Research Institute https://otworywiertnicze.pgi.gov.pl. Unfortunately, a complex geological setting, including tectonic deformations and limited exposure of the deposits of the Ropianka Fm, limited the detail and completeness of the facies map prepared.

SEDIMENTARY FACIES

The sedimentary succession studied includes various lithologies, from mudstone and marlstone to siltstone, sandstone, and conglomerates, which are descriptively characterised and classified as 11 sedimentary facies. The sedimentary facies are distinguished on the basis of bed thickness, textural properties, primary depositional and erosional structures, lower and upper bedding surfaces and deformational structures, and interpreted in terms of their depositional processes.

The sandstones are whitish, yellowish, and rusty-orange to grey in colour, calcareous to noncalcareous quartz arenite to sublitharenite, strongly to poorly cemented, which is a characteristic feature of the Ropianka Fm (Bromowicz, 1974). Some of the sandstone beds change colour from brown, dark grey to almost black, owing to scattered carbonised plant detritus, coal and tiny clasts of dark mudstone, grey to dark grey, owing to increased dispersed mud, or rarely greenish, owing to scattered glauconite. Minor petrographic components are represented by mud and marl chips, carbonised plant detritus, muscovite and biotite flakes, glauconite, feldspar, pyrite, agglutinated foraminifer tests, peloids and other fragmented bioclasts. Exotic components are represented by coal, siliceous rocks, greenschist, igneous rocks (granitoid, pegmatite) and volcanic rocks (rhyolite, andesite), sandstones, and Štramberk-type limestones. In general, the lithological composition of the exotics is similar to that reported in the Upper Cretaceous of the Silesian Nappe (Strzeboński *et al.*, 2017) and the Skole Nappe (Łapcik *et al.*, 2016; Łapcik, 2019). However, detailed petrographic analysis of the exotic material was not the aim of the study.

Facies F1: Massive graded and ungraded conglomerate and sandstone

Description: Facies F1 consists of coarse- and medium- to fine-grained sandstone, rarely with a granule-to-cobble conglomeratic base (Fig. 3A) and thickness between 2.5 and 262 cm (mean ~43.7 cm). The conglomeratic base is predominantly thinner than the sandy part above. However, some pure conglomerate beds also occur. Facies F1 shows sharp, erosional to flat bases with sole marks and rare load
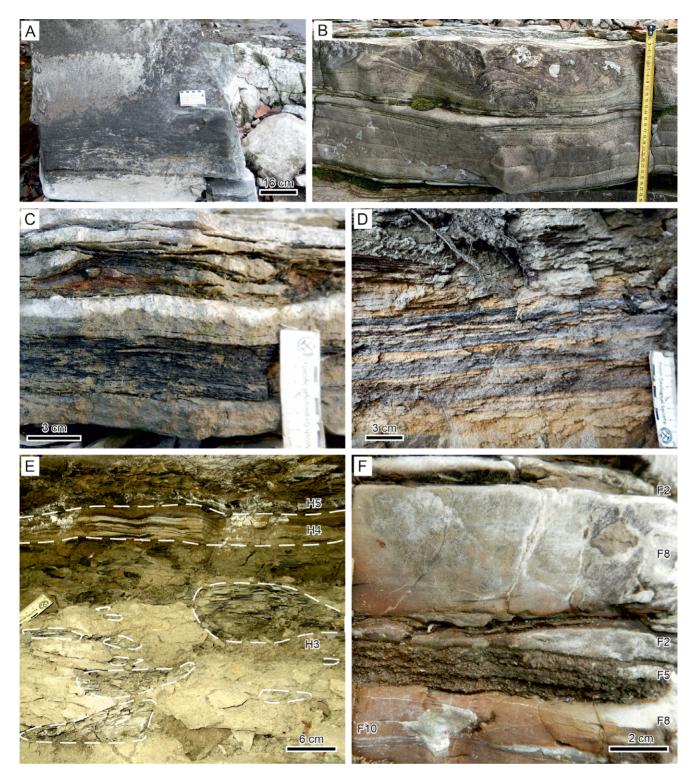
Fig. 3. Outcrop examples of facies F1–F5. **A.** Massive sandstone of facies F1 with dewatering structures near its base, Dunajec section. **B.** Structured sandstone of facies F2 with planar-parallel lamination, ripple cross-lamination, and convolute lamination, Dunajec section. Note repetitive divisions with planar-parallel and ripple cross-lamination. **C.** Banded sandstone of facies F3 with dark bands, up to 4 cm thick, enriched in coalified plant detritus and mud chips, Dunajec section. **D.** Banded division of facies F3 with multiple alternations of dark and light bands. The thickness of dark bands decreases towards the top of the bed, Janowice section. **E.** Clast-rich sandstone division of facies F4, which is considered as an H3 division (*sensu* Haughton *et al.*, 2009) capped with ripple cross-laminated sandstone, enriched in coalified plant detritus (facies F3), considered as H4 division (*sensu* Haughton *et al.* (2009), Janowice section. Note the upward increase in the muddiness of H3 division matrix and the increase in the contribution of small mudclasts (only larger clasts are marked with the white, dashed line in the lower part of the H3 division). Massive sandstone (facies F1) below the H4 is not captured in the picture. **F.** Alternation of facies; from the bottom upwards: heterolithic deposits (F10) and marlstone (F8) capped by a thin layer of coarse-grained lag deposits of facies F5 with abrupt grains-size break to facies F2, indicating sediment bypass. Further interbedding of facies F2 and F8 occurs up the section, Dunajec section.

features. Sole marks are represented by trace fossils, scour marks (flutes), and tool marks (groove marks and rare occurrences of skim and prod marks). The recognised trace fossils include *Ophiomorpha* isp., *Ophiomorpha annulata*, *Scolicia* isp., *Scolicia strozzii,* and *Thalassinoides* isp. Massive sandstones very rarely contain epichnia and endichnia bioturbation structures, usually *Ophiomorpha annulata*. Facies F1 is dominated by graded and massive divisions, but can show dewatering structures, i.e., dish, plate, and pillar structures. The coarse fraction occurs as normal-distribution grading, coarse-tail grading, and as scattered larger grains within the finer-grained matrix. Grain-size analysis shows that at least some beds of the macroscopically massive sandstone are graded and inversely graded (Supplementary Material, Table S1). Grain-size breaks and small- to medium-sized erosional features indicate surfaces of amalgamation. Moreover, remarkably pronounced grain-size breaks may occur between facies, as they transition from facies F1 to F2 and F3 (described below). Intraformational clasts of grey, black, and green mudstone and bluish-white marlstone, as well as coal clasts, are relatively common. These clasts are orientated parallel to the bedding and are concentrated mostly in discrete horizons at the base and/or top of the structureless sandstone. Their size varies and reaches up to 24 x 2.5 cm (mudstone and marlstone clasts), but rarely exceeds a few centimetres. Some of the intraformational clasts show similarities to facies F7 and F8 (described further). Granule- to pebble-sized clasts of various exotics occur mostly in the coarsest fraction.

Interpretation: The massive graded division of facies F1 was formed as a result of rapid suspension fallout from highly concentrated gravity flows (Kneller and Branney, 1995) and corresponds to the turbidite division T_a of Bouma (1962) and division S_3 of Lowe (1982). Such deposits are formed by the nontractional damping of near-bed turbulence with a high aggradation rate (Arnott and Hand, 1989; Leclair and Arnott, 2005; Talling *et al.*, 2012). Some of the massive fine-grained macroscopically ungraded sandstone beds show fractional grading in grain-size analysis and therefore indicate settling from a well-sorted sandy turbulent gravity flow (Pickering and Hiscott, 2015). Grain-size breaks, occurring within facies F1 and in its transition to the superposed facies F2 or F3, are direct evidence of flow bypass and relative proximity of the depositional setting (Stevenson *et al.*, 2014; Tinterri *et al.*, 2017). Dewatering structures correspond to syn- and postdepositional liquefaction, due to a high aggradation rate (Stow and Johansson, 2000).

Macroscopically graded and ungraded massive divisions can also be formed by the repeated collapse of laminar shear layers (Sumner *et al.*, 2008, 2009; Talling *et al.*, 2012) and a liquified layer with excess pore pressures (Ilstad *et al.*, 2004). Last, but not least, it cannot be excluded that some of the massive ungraded sandy deposits, especially with groove marks at their base, also may have been formed by *en masse* deposition from sandy gravity flows, dominated by laminar flow behaviour (cf. Shanmugam and Moiola, 1995; Talling *et al.*, 2012; Strzeboński, 2015, 2022; Peakall *et al.*, 2020).

Facies F2: Structured sandstone and conglomerate

Description: Facies F2 consists of very-fine to coarse-grained sandstone, rarely gravelly sandstone, or granule to pebble conglomerate (Fig. 3B). The thickness of the structured sandstone ranges from <1 cm to 217 cm (mean ~10.5 cm). Beds of facies F2 are predominantly tabular, but beds thinner than 10 cm may be lenticular, with lateral pinch-outs. The sharp base of a structured sandstone is flat to erosive, uneven or deformed by load structures. In some cases, a gradational base occurs, where the sandstone is underlain by facies F1. The soles of beds are dominated by trace fossils, but flute, groove, skim and prod marks also occur. Usually, one type of sole mark predominates, but trace fossils, scour marks and tool marks may co-occur. A structured sandstone is predominantly graded, sometimes with scattered grains of coarse-grained sand or granules or amalgamation surfaces, recorded as grain-size breaks. Internal sedimentary structures include plane-parallel lamination, low-angle lamination, ripple cross-lamination, climbing-ripple cross-lamination, and very rarely large-scale cross-lamination (>4 cm high). Some of the laminae are given greater prominence by a higher contribution of dispersed carbonised plant detritus, coal and tiny mud chips. The internal sedimentary structures may have been deformed plastically by the dewatering process and show wavy and convolute lamination. Beds, mostly up to a few centimetres thick, entirely consisting of ripple cross-laminae and/or low-angle laminae, are not uncommon. Besides common ripple cross-lamination, such beds may include climbing ripple marks and ripple marks deformed by loading. In addition, these beds often show bedform morphology reflecting the primary shape of ripple marks, with both stoss and lee sides preserved. Mudstone and marlstone clasts (up to 24 x 5 cm in size) tend to be concentrated at the bases or tops of the beds and usually are oriented parallel to the bedding. Some of the thin-bedded sandstones contain scattered chips of mudstone, no larger than a few millimetres, and the same beds frequently show a higher proportion of dispersed mud. A higher content of these mud chips occurs in the banded sandstones of facies F3. Coarse-grained and conglomeratic structured sandstone may include exotic components, which are the same as those in facies F1. The top of facies F2 usually gradually passes into or shows a sharp boundary with the banded sandstone (facies F3), heterolithic deposits (facies F10), mudstone (facies F7) or marlstone (facies F8) occurring above. Trace fossils occur primarily as hypichnia, but endichnia and epichnia also are present. Some of the facies F2 beds are poorly laminated, owing to homogenization by bioturbation. Identified trace fossils include *Ophiomorpha* isp., *Ophiomorpha annulata*, *Cosmorhaphe* isp., *Scolicia* isp., *Scolicia strozzii, Thalassinoides* isp. and *Capodistria* isp.

Interpretation: The structured sandstone corresponds to the divisions $T_{bc(d)}$ of Bouma (1962) and the T_t division of Lowe (1982), formed under conditions of deposition from traction with a relatively low fallout rate and represents the phase of lower-density fully turbulent flow, predominantly in a waning surge-type turbidity current (Talling *et al.*, 2012). In such conditions, tractional sedimentary structures are generated, i.e., plane-parallel lamination and ripple cross-lamination

(Allen, 1982; Best and Bridge, 1992). Plane-parallel lamination may also be the result of deposition from a traction carpet (spaced stratification; cf. Hiscott and Middleton, 1980; Lowe, 1982; Sumner *et al.*, 2008; Cartigny *et al.*, 2013). During this phase of the flow, brief episodes of bypass and substrate reworking are possible (e.g., Sumner *et al.*, 2008; Talling *et al.*, 2012; Stevenson *et al.*, 2014; Tinterri *et al.*, 2017). Wavy and convolute lamination are interpreted as syn- and postdepositional soft-sediment deformation, due to partial sediment liquefaction (Dżułyński, 1996, 2001; Owen *et al.*, 2011).

Facies F3: Banded sandstone

Description: Facies F3 consists of distinctive fine to very fine-grained brown and black bands and laminae, which are enriched in coalified plant detritus and coal clasts up to pebble-size, mica flakes, and small chips of grey mudstone (Fig. 3C, D). Dark bands are massive or planar-parallel laminated and interbedded with yellowish to whitish, plane-parallel laminated and/or ripple cross-laminated to structureless bands of 'clean sand'. A particular sandstone bed may include up to a dozen couplets of dark-light bands. Dark and light bands may have similar thicknesses, or either type may predominate. Band thickness ranges from micro- to mesobanding, with very few exceptions of macrobanding (Lowe and Guy, 2000). Sandstone of facies F3 very rarely occurs as a separate bed and is mainly a part of a thicker bed, where it generally co-occurs with facies F1 and/or F2. Facies F3 may occur at different heights in the sandstone bed; however, it is mainly concentrated at the top of such beds. The thickness of facies F3 ranges from 1.5 to 67.5 cm (mean ~14.6 cm). Some of the bands are plastically deformed and show convolution, wave-shaped deformation, or are replaced with irregular bodies and lenses, enriched in coalified plant detritus and coal clasts. In both cases, this plastically deformed division occurs mostly in one bed, just above a sandstone of facies F1, containing dewatering structures. The sandstones of facies F3 tend to show a gradual decrease in grain size up to a silty and muddy, laminated top or a sharp top with sandy mudstone or clayey mudstone above. Larger clasts of coalified plant debris may include rare *Teredolites* isp.

Interpretation: A facies of this type implies internal flow pulses with a depositional mode occurring between two end members, i.e., turbidity current and debris flow (cf. Lowe and Guy, 2000; Lowe *et al.*, 2003; Baas *et al.*, 2009; Haughton *et al.*, 2009; Stevenson *et al.*, 2020; Łapcik, 2023). Turbulent flow is represented by tractional deposition and the appearance of ripple and planar-parallel lamination. Transitional to laminar flow conditions are reflected in dark bands. Stevenson *et al.* (2020) link the banding formation conditions with those required for the generation of planar-laminated (Bouma division T_b) sandstone, but beneath mud-laden transitional plug flows that control the final product, mostly by a different content of cohesive mud in the flow. Occurrences of soft-sediment deformation imply a relatively high aggradation rate or are caused by the reduced permeability of the mud-rich bands.

Facies F4: Structureless muddy sandstone and clast-rich sandstone

Description: Facies F4 consists of very fine- to medium-grained sandstone, more rarely with scattered coarse grains, and thicknesses ranging from 2 to 175 cm (mean ~45.6 cm). The base and top surfaces of facies F4 are mostly sharp and flat. The sandy matrix of this macroscopically structureless and ungraded sandstone commonly shows a grey hue, indicating a higher proportion of dispersed mud. Muddy sandstone may bear a relatively high proportion of intraformational clasts of mudstone (facies F7) and marlstone (facies F8), which are chaotically dispersed in the matrix-supported background sediment (Fig. 3E). Additionally, randomly scattered brown to black irregular bodies, enriched in coalified plant detritus and coal, may occur. Facies F4 occurs as independent beds or complex beds, where it is underlain by the massive sandstone of facies F1 or the structured sandstone of facies F2. In the second case, facies F4 occasionally is capped by structured sandstone of facies F2 or banded sandstone of facies F3.

Interpretation: This facies is interpreted as the deposit of a poorly cohesive to cohesive sandy debris flow, deposited by *en masse* cohesive freezing (Talling *et al.*, 2012). It is plausible that the parental turbulence-dominated gravity flow was transformed by incorporation of cohesive mud from an eroded substratum and partly disintegrated mud clasts, which resulted in cohesive bulking (cf. Fisher, 1983; Haughton *et al.*, 2003, 2009; Fonnesu *et al.*, 2016). The processes of flow deceleraion, favoured by the tectonically controlled morphologic controls, also may have played an important role in the flow transformation (Tinterri *et al.*, 2016, 2020). In some cases, facies F4 occurs directly above facies F1 and therefore it is considered to have been part of a hybrid event bed (HEB) and corresponds to division H3 of Haughton *et al.* (2009), whereas the sandstones of facies F2 and F3 at the top correspond to division H4. Such deposits are interpreted as having been generated from strongly stratified transitional flows (Baas *et al.*, 2011; Kane and Pontén, 2012; Talling, 2013; Kane *et al.*, 2017; Fonnesu *et al.*, 2018) or from the cogenetic turbidity currents (lower division) and cohesive debris flows (upper division) of Haughton *et al.* (2003, 2009); and Hodgson, (2009).

Facies F5: Lag deposits

Description: Facies F5 is characterised by medium- to very coarse-grained sandstone and granule conglomerate, organised into very thin to medium beds and layers, with thicknesses ranging from ~0.3 cm to 12 cm (mean ~2.5 cm). Grains of various exotic material, millimetre-scale mud chips and biogenic material, mixed with quartz grains are common. Facies F5 always exhibits a contrast in grain size with respect to the surrounding muddy or marly fine-grained deposits (Fig. 3F), showing the "type I grain-size breaks" of Stevenson *et al.* (2014). However, the coarse-grained part may be capped with marlstone or mudstone, instead of fine-grained sand. These beds invariably show a sharp and flat to undulated erosive base, rarely with load structures or flute marks, and a sharp top, which may be flat to uneven. Lateral

continuity of the beds and layers is variable and may change from a layer, a few metres long, to lenses a few centimetres long, with lateral pinch-outs. The same bed may change laterally from a convex-down shape (undulating erosive bottom) to a small convex-up shape (bedform morphology). Beds of facies F5 are massive to planar-parallel, low-angle, and cross-laminated. Some of the beds of facies F5 represent clast-rich conglomerates. Clasts are predominantly represented by mudstone (facies F7) and marlstone (facies F8) that reach up to several centimetres along their longest axis. The coarse material from the beds of facies F5 can be concentrated in burrows, formed in the surrounding fine-grained deposits of facies F7 and F8. The small thickness of the bed and the surrounding fine-grained deposits is the main difference between this facies, F5, and beds composed of facies F1 and F2.

Interpretation: Facies F5 is interpreted as the isolated lag deposits of partially bypassing highly concentrated flows, mostly of a turbulent nature (cf. Mutti, 1992; Stevenson *et al.*, 2014, 2015; Cunha *et al.*, 2017; Tinterri *et al.*, 2017; Brooks *et al.*, 2018). Some of these flows were erosive and left scoured surfaces, which were filled with the coarse-grained deposits of facies F5. The unstable nature of the flow and its heterogeneous internal structure on a scale of centimetres to tens of centimetres is recorded by the discontinuous distribution of the coarse-grained material and erosional structures. Such lag deposits were formed in a proximal area, where bypassing flow capacity was enough to suspend most of the sediment load, but a slight reduction in flow competence resulted in the fallout of its coarsest fraction (cf. Mutti and Normark, 1987). Therefore, facies F5 is considered to be a more proximal equivalent of facies F1 and F2. In some cases, these lag deposits may have been reworked by the same or a subsequent strongly turbulent flow that generated small bedforms. Rarely, solitary trace fossils filled with coarse grains are the only evidence for the presence of a previous thin lag lamina that was reworked by the activity of benthic infauna.

Facies F6: Dune-scale cross-laminated sandstone

Description: This subordinate facies F6 consists of fine- to coarse-grained sandstone and pebbly sandstone, organised into highly uneven, lenticular beds (Fig. 4A, B). These beds, with thicknesses ranging from 4.1 to 48 cm (mean 12.7 cm), may laterally pinch out on the scale of an outcrop. The bases and tops of facies F6 are sharp. Beds of facies F6 show dune-scale cross-lamination and may contain abundant clasts of mudstone and marlstone, as well as exotic grains and pebbles. This facies occurs in sections, dominated by marlstone of facies F8 and like facies F5 shows a high contrast with the fine-grained surrounding deposits in the same section.

Interpretation: Facies F6 is interpreted as dune bedforms, generated under sustained and fully turbulent flow with a low rate of suspended fallout (Allen, 1982; Southard, 1991). Like facies F5, these bedforms represent lag deposits in close proximity to the erosion area, reworked under the strong sustained and mostly bypassing sediment gravity flow in the proximal area, or they may be the remnants of a former sand bed, reworked by a bypassing fully turbulent

flow (cf. Mutti and Normark, 1987; Mutti, 1992; Amy *et al.*, 2000, 2007; Gardner *et al.*, 2003; Stevenson *et al.*, 2015; Cunha *et al.*, 2017; Tinterri *et al.*, 2017). Clast-rich beds are evidence for the up-dip erosion of the muddy substratum. The significant contrast in grain size with the surrounding mostly fine-grained marly substratum is a result of the high efficiency of sediment gravity flows, which deposited only their coarsest fraction.

Facies F7: Mudstone

Description: Facies F7 consists of grey to dark grey, greenish, brownish, reddish, and variegated mudstone (Fig. 4C). The mudstone beds are calcareous to noncalcareous, with thicknesses between 0.1 and ~50 cm (mean 2.4 cm), although an exceptionally long interval reaching ~10 m thick was observed. Facies F7 represents silty and sandy mudstone and clayey mudstone. These layers have gradational, rarely sharp bases and mostly sharp tops. Facies F7 is massive, poorly laminated or mottled with rare to abundant bioturbation structures, mostly *Chondrites* isp., *Planolites* isp. and *Ophiomorpha* isp. Very rarely, internal surfaces with mud ripples were observed. In the case of thin intercalations of sandy and silty laminae with mud, such deposits were classified as the heterolithic deposits of facies F10. The biogenic components of the mudstone are represented by calcareous nannoplankton, the tests of foraminifers, diatoms and radiolarians, echinoderm spicules, fish teeth, and coalified plant detritus. Very rarely, *Inoceramus* shells are observed, mostly in a life position, with both valves preserved. Non-biogenic components are dominated by clay minerals and quartz, with an admixture of lithic grains, carbonates, muscovite, glauconite, and pyrite.

Interpretation: A clear distinction of the depositional process of facies F7, based mostly on macroscopic features, remains difficult. The sandy and silty mudstone of facies F7 is interpreted as deposits formed under conditions, where the sand and silt grains were not segregated from the clay particles during deposition. This may indicate a dilute fine-grained sediment gravity flow, where the cohesive force prevents grain segregation and represents the deposits of upper transitional plug flows and quasi-laminar plug flows, which may have evolved from fully turbulent flow (Baas *et al.*, 2011). On the other hand, clay can be transported, together with silt and sand, as non-cohesive or poorly cohesive flocculated mud or rip-up aggregates in the stable velocity / shear stress range (Schieber *et al.*, 2010, 2019 and references therein). Graded mudstone is a product, formed by a mud-rich fragment of a low-density turbidity current (cf. Talling *et al.*, 2012). Clayey mudstone is interpreted as sediment, deposited from the final settling phase by dilute sediment gravity flows, hemipelagic 'background' sedimentation, or the lateral transport of hemipelagic deposits by ocean currents and/or aeolian action (Talling *et al.*, 2012; Pickering and Hiscott, 2015). Last, but not least, massive mudstone beds may correspond to sediment gravity flows of fluidal mud (Baas *et al.*, 2009). The mudstone of facies F7 is variably calcareous and therefore indicates sedimentation in changing conditions, above or close to the local lysocline depth. The variable degree of bioturbation and colour
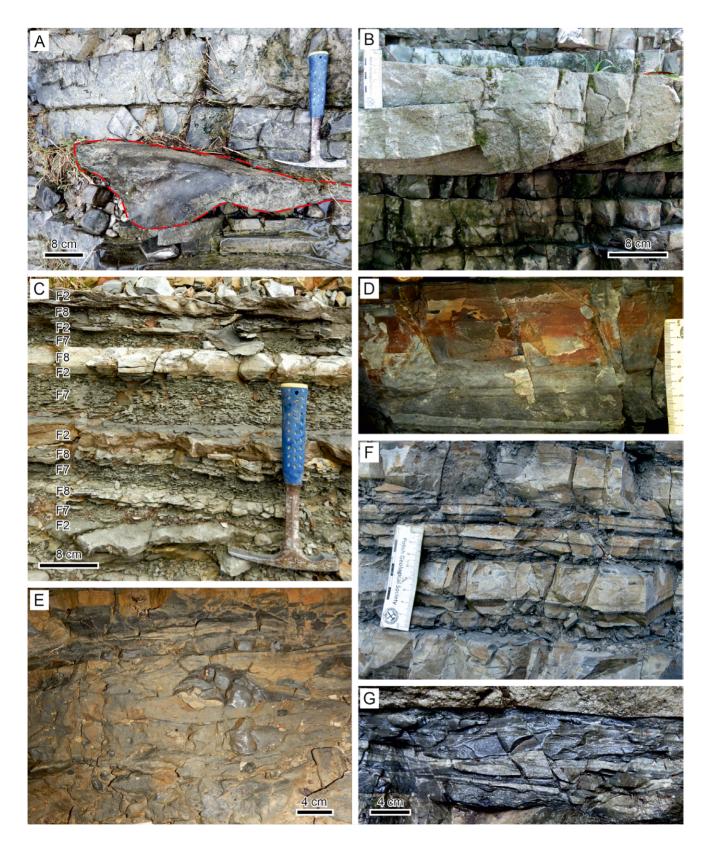
Fig. 4. Outcrop examples of facies F6–F11. **A.** Large-scale cross-laminated dune (3D bedform) of facies F6 (marked with a red, dashed line), interbedded with marlstone beds of facies F8, Dunajec section. **B.** Dune-scale cross-bedding of facies F6 interbedded with marlstone beds of facies F8, Szczepanowice section. **C.** Interbedding of mudstone of facies F7, marlstone of facies F8 and thin-bedded sandstone with convolute lamination of facies F2, Dunajec section. **D.** Marlstone bed of facies F8 with siltstone of facies F9 at the base, Szczepanowice section. **E.** Matrix-supported clast-rich conglomerate of facies F11, dominated by intrabasinal material, Zagórze section. **F.** Interbedding of thin-bedded bioturbated marlstone of facies F8 and thin layers of dark mudstone of facies F7, Szczepanowice section. **G.** Mud-dominated heterolithic deposits of facies F10 with thin laminae of siltstone and very fine-grained sandstone and varied bedforms, showing cross-bedding and low-angle lamination, Lubinka section.

indicates an environment with changing oxygenation and nutrient supply on the seafloor.

Facies F8: Marlstone

Description: This type of facies is represented by bluish white and light-grey marlstone (Fig. 4C, F) with bed thicknesses ranging from 0.2 to 37.5 cm (mean thickness ~4.44 cm). Locally, marlstone is grey to dark grey, greenish, beige, and reddish in colour. Marlstone occurs as strongly silicified beds to soft shaley layers. The bases of the beds are mostly sharp, where they are underlain by siltstone and sandstone, or sharp to gradual, where underlain with mudstone. The tops of the beds are sharp to erosional, if overlain by sandstone and siltstone, and sharp to gradual, where they are covered with mudstone. In the outcrop, the marlstone is predominantly massive, with abundant bioturbation structures. However, on cut surfaces and in thin sections, it may show grading and poorly preserved parallel-laminated marlstone and light-coloured silty/sandy laminae, which are very similar to the colour of the marlstone. Marlstone with numerous intercalations of sandy/silty laminae is classified as a heterolithic deposit of facies F10. The burrows are filled predominantly with dark muddy material, although some of them are filled with silty, sandy and even gravelly grains from the beds overlying or underlying the marlstone, respectively. The coarsest grains may be concentrated in the trace fossils. Recognised trace fossils are commonly represented by *Chondrites* isp. *Chondrites affinis*, *Chondrites intricatus*, *Planolites* isp., *Ophiomorpha* isp., and *Scolicia* isp. More rarely, *Thalassinoides* isp., *Zoophycos* isp.*, Helminthoida* isp., *Alcyonidiopsis* isp., and ?*Squamichnus acinaceformis* occur. The number of burrows usually increases upward in particular beds, especially in the thicker beds (>5 cm). The biogenic components of the marlstone are represented by calcareous nannoplankton, tests of foraminifer and more rarely ostracods, fish teeth, coalified plant detritus, and fragments of *Inoceramus* shells; as well, echinoderm and sponge spicules may occur. Non-biogenic components are dominated by micrite and quartz grains, with a minor proportion of pyrite, lithic grains, glauconite grains, and muscovite flakes. In the poorly exposed or less accessible parts of the outcrops, a grey type of facies F8 is difficult to distinguish from the calcareous mudstone of facies F7, which may show a similar colour.

Interpretation: The marlstone beds are interpreted as the deposits of highly dilute, muddy calciturbiditic currents (cf. Stow and Bowen, 1978, 1980; Leszczyński *et al.*, 1995; Leszczyński, 2003, 2004). They plausibly represent deposits, formed in the same way as the classic Bouma divisions T_{de} under tractional and suspension fallout conditions. Very poor lamination and the massive structure of beds are most likely the result of homogenisation by bioturbation and the very narrow distribution of grain size. Some of the massive beds with a paucity of silt and sand grains may originate from gravity flows of fluidal mud (Baas *et al.*, 2009). The beds of facies F8 may have been deposited slowly from suspension as hemipelagites. However, the co-occurrence of marlstone with the noncalcareous mudstone of facies F7 in one section implies an interpretation of them as the products of sediment gravity flow. The high contribution of bioturbation structures and the significantly higher diversity of ichnospecies indicate good seafloor conditions for benthic life, with a higher oxygen content and a greater supply of nutrients than in the case of the mudstone facies F7.

Facies F9: Siltstone and very fine-grained sandstone

Description: Facies F9 is represented by thin beds and laminae of whitish, yellowish, and grey siltstone (Fig. 4D), the thickness of which ranges from 0.1 to 7 cm (with mean ~0.7 cm). Siltstone beds and laminae can contain admixtures of very fine-grained sand to fine-grained sand, which are usually dominated by foraminifera tests and other bioclastic components. Sand-sized grains may also be represented by quartz, carbonised plant detritus, glauconite, mica flakes and small mud chips. The lower surfaces are predominantly sharp and flat, with sole marks dominated by trace fossils. The top of facies F9 is sharp and flat, rarely gradational. The siltstone is graded (on a microscale) to ungraded and structureless, but it can also show planar-parallel lamination, low-angle lamination, and cross-lamination. Sedimentary structures may be deformed by water escape into the wavy or more chaotic laminae or by bioturbation. The siltstone facies F9 occurs abundantly as the lower part of the marlstone beds of facies F8 and more rarely as the bottom deposits of the mudstone of facies F7.

Interpretation: This type of facies is interpreted as having been generated by fine-grained dilute and fully turbulent sediment gravity flows or lower transitional plug flows (Leszczyński *et al.*, 1995; Leszczyński, 2003, 2004; Baas *et al.*, 2011). During such deposition, silt-sized grains freely settled out of suspension, and traction structures were formed (Piper *et al.*, 1984; Talling *et al.*, 2012). The abundance of biogenic grains points to pelagic deposition. However, the admixture of scattered terrigenous material (quartz grains, glauconite, plant detritus, and exotic grains) indicates an origin as material, redeposited from a shallower area (Scheiber *et al.*, 2019). The deposits of facies F9 mainly represent the lower division of low-density calcareous turbidites with the marlstone of facies F8 at the top. Some of the structureless siltstone beds may have originated as deposits homogenised by bioturbation.

Facies F10: Heterolithic deposits

Description: Facies F10 occurs as a siltstone and very fine-grained sandstone, intercalated with calcareous to noncalcareous mudstone or marlstone in three hierarchical tiers: 1) single layers and laminae of siltstone/sandstone and mudstone/marlstone; 2) heterolithic divisions with specific structural and textural properties; and 3) heterolithic intervals, composed of one or more of the heterolithic divisions as products of individual sediment gravity-flow events. This concept of deep-water heterolithic deposits is described in detail in Łapcik (2023). The heterolithic intervals are up to 15.8 cm thick. Individual laminae are mainly up to a few millimetres thick, sometimes with a pinch-and-swell geometry. Commonly, the proportion of siltstone to mudstone decreases upwards in terms of the thickness of laminae

(Fig. 4G). The boundaries between the siltstone and mudstone laminae are sharp, with local load structures, erosional surfaces, flame structures and bioturbation structures (endichnia and hypichnia). Trace fossils are similar to those, identified in the mudstones of facies F7 and the marlstones of facies F8. Sandstone and siltstone beds are graded to ungraded and show internal plane-parallel lamination, wavy lamination, low-amplitude bed-waves, ripple cross-lamination, and climbing-ripple cross-lamination, commonly with mud/marl drapes or mud/marl streaks. Some of the beds are laterally discontinuous and contain starved and/or loaded ripples. Heterolithic divisions represent all types from A1 to A9, described by Łapcik (2023), but their detailed characteristics are not the aim of this article.

Interpretation: Possible interpretations of the heterolithic deposits are numerous. However, similarities of the deposits studied to the heterolithic deposits, described in the Veřovice and Lhoty Fms of the Silesian Basin, indicate their origin as turbulent and transitional flows with a tendency to form pulsating unsteady waxing and waning flows in the deposits of a relatively proximal area (cf. Łapcik, 2023 and references therein).

Facies F11: Pebbly mudstone and massive muddy conglomerate

Description: This facies includes beds of pebbly mudstone and massive muddy conglomerate, with thicknesses ranging from 2.5 to 260 cm (mean ~111.4 cm). Facies F11 shows sharp bases with rare loading and sharp tops with flat to uneven surfaces as well as rare load and erosional features. Beds are nongraded, matrix-supported with randomly dispersed granule- to cobble-size (rarely boulder-size) material of exotic origin and intraformational debris of mudstone, marlstone, heterolithics, siltstone, and sandstone, representing ripped-up fragments of the previously described facies (Fig. 4E). The conglomeratic fraction may show both plastic and brittle deformation. Even in one bed, the calcareous to noncalcareous matrix may locally pass from sand- to mud-dominated. Beds of facies F11 may be dominated by exotic material, dominated by intraformational clasts, or be composed of a mix of both types of material. In general, intraformational clasts are mostly subrounded, whereas exotic clasts are rounded. This type of deposit is concentrated in the southern area, especially in the uppermost parts of the Zagórze and Lichwin sections.

Interpretation: This type of facies is interpreted as the deposits of cohesion-dominated debris flows, characterised by *en mass* deposition, due to cohesive freezing (Talling *et al.*, 2012; Pickering and Hiscott, 2015; Strzeboński *et al.*, 2017; Strzeboński, 2022). The beds of facies F11 with boulders of intraformational clasts correspond to the early stages of a flow transformation from initial slumps to debris flows. The type of deformation (plastic vs brittle) indicates the degree of lithification of the components transported and the scale of internal shear during the mass transport event. The facies transition from facies F1 to F11, which like the transition from facies F1 to facies F4 indicates 'linked debrite' and therefore is interpreted as division H3 of HEB (Haughton *et al.*, 2003, 2009). In this case, there is an important

difference in sand-to-mud ratio between facies F4 and F11 and the common presence of exotic clasts. This difference may have promoted the transformation of the parental debris flow into a bipartite hybrid flow, leading to dilution of the debris flow head and separation of the outrunning high-density turbidity current (e.g., Haughton *et al.*, 2009).

FACIES ASSOCIATIONS

The sedimentary facies characterised above have been grouped into seven facies associations (FA), which occur as packages, up to tens of metres thick. These facies groups have been distinguished on the basis of differences in facies composition, the mean, median and variance of bed thicknesses, upward grain-size trend, sandstone net-to-gross percentage and vertical facies transition (see data summary in Table 1), as well as comparison with the deposits of the Ropianka Fm in the western part of the Skole Basin (Łapcik, 2017, 2018, 2019). Facies, for which the contribution to a particular facies association (FA) is <1%, are considered as subordinate and are not mentioned in the text, but still are listed in detail in Table 1. The individual FAs are interpreted as different morphodynamic sub-environments of the submarine depositional system. They are representatives of the well-established architectural element concept in the submarine depositional system, the main signatures and characteristics of which are described in areas that are better exposed and less tectonically deformed (e.g., Spychala *et al.*, 2017; Brooks *et al.*, 2018; Fonnesu *et al.*, 2018; Hansen *et al.*, 2019). The first two facies associations (FA1 and FA2) are strongly dominated by carbonate deposits, whereas the remaining five facies associations (FA3–FA7) are arranged in order, characterised by a gradual decreases in grain size, sand-mud ratio, and bed thickness, reflecting a shift toward a less energetic depositional environment of the turbidite system.

Facies association 1 (FA1): Marlstone-dominated lower-slope and base-of-slope deposits

Description: This facies association (FA1) is strongly dominated by fine-grained deposits (sandstone net-to-gross of 0% to 21%) with a significantly higher proportion of marlstone (62.9% of facies F8) over mudstone (21.3% of facies F7; Fig. 5). Sandstone facies contribute 8.6%, with the predominance of facies F2 (7.9%) and sandstone bed thicknesses range between 1 and 217 cm with the significant predominance of thin beds (sandstone mean = 5.2 cm; median = 2.8 cm). Solitary thin- to thick-bedded sandstone is very rarely distributed within the marl-dominated sections. Heterolithic deposits (F10 5.2%) and siltstone (F9 2%) have fourth and fifth place in the overall percentage composition of FA1, but their proportions may have been underestimated, owing to their poor contrast with marlstone. The packages of FA1 range from 0.9 to 41.7 m in thickness (mean ~12.5 m) and show almost exclusively thin-bedded logs without the characteristic grain-size and bed thickness trends. Despite the predominance of tabular beds, there are beds with undular morphology and erosional features.

Quantitative summary of the characteristics of facies associations in the study area.
Note colour code of the facies and facies associations in Table 1
according to the legends in Figures 7 and 10, respectively.

Marlstone-dominated lower-slope and base-of-slope FA1		Marlstone-dominated lower-slope and base-of-slope bypass zone FA2		Channel-fill deposits and channel-lobe transition zone FA3		Lobe-axis deposits FA4		Lobe-off-axis deposits FA5		Lobe-fringe deposits FA6		Interlobe deposits / lobe-distal-fringe deposits FA7	
Package thickness 0.9–41.7 m (mean 12.5 m)		Package thickness 2–21.6 m (mean 9.8 m)		Package thickness 5.6–36.6 m (mean 17.7 m)		Package thickness 3–9.3 m (mean 5.4 m)		Package thickness 1.7–19.5 m (mean 6 m)		Package thickness 0.8–5.7 m (mean 3.1 m)		Package thickness 0.8–5.5 m (mean 2.9 m)	
Component facies thickness contribution:	Individual facies bed thicknesses:	Component facies thickness contribution:	Individual facies bed thicknesses:	Component facies thickness contribution:	Individual facies bed thicknesses:	Component facies thickness contribution:	Individual facies bed thicknesses:	Component facies thickness contribution:	Individual facies bed thicknesses:	Component facies thickness contribution:	Individual facies bed thicknesses:	Component facies thickness contribution	Individual facies bed thicknesses:
F8 62.88%	0.2–36 cm (mean 4.4 cm)	F8 56.74%	0.5–37.5 cm (mean 5.2 cm)	F1 40.58%	2.5–150 cm (mean 55.6 cm)	F1 73.67%	3.5–262 cm (mean 59.8 cm)	F2 45.24%	1–113 cm (mean 18.3 cm)	F2 36.06%	1–55 cm (mean 6.4 cm)	F7 29.69%	0.1–22 cm (mean 3.1 cm)
F7 21.34%	0.1–50 cm (mean 1.8 cm)	F7 16.14%	0.1–20 cm (mean 2 cm)	F2 23.49%	1–142 cm (mean 30.4 cm)	F2 10.33%	1–68.5 cm (mean 19.5 cm)	F1 16.53%	4–60 cm (mean 20.8 cm)	F7 30.93%	0.3–30 cm (mean 3.3 cm)	F8 27.31%	0.8–13.5 cm (mean 3.1 cm)
F2 7.94%	1–217 cm (mean 5.2 cm)	F2 9.94%	0.7–20 cm (mean 3.4 cm)	F4 14.45%	6–175 cm (mean 69.3 cm)	F4 5.6%	3–150 cm (mean 59.9 cm)	F3 12.96%	2–67.5 cm (mean 19.8 cm)	F3 14.15%	2–61 cm (mean 14.6 cm)	F2 22.72%	1.5–3 0.5 cm (mean 5.9 cm)
F10 5.19%	0.3–14.3 cm (mean 1.9 cm)	F5 4.37%	0.3–11.8 cm (mean 2.2 cm)	F11 12.21%	2.5–159 cm (mean 97.6 cm)	F3 4.6%	1.5–46.5 cm (mean 10 cm)	F7 10.83%	0.5–35.5 cm (mean 4.7 cm)	F1 8.35%	2.5–38 cm (mean 12.1 cm)	F10 8.48%	0.7–12.7 cm (mean 3.6 cm)
F9 1.98%	0.1–7 cm (mean 0.5 cm)	F10 4.24%	0.5–15.8 cm (mean 2.9 cm)	F3 6.25%	0.6–64 cm (mean 21.4 cm)	F11 2.89%	10–260 cm (mean 135 cm)	F11 9.04%	59–248 cm (mean 117.3 cm)	F8 4.48%	0.8–15 cm (mean 3.4 cm)	F3 7.16%	1.5–13.5 cm (mean 8 cm)
F3 0.26%	1.5–8 cm (mean 4.7 cm)	F6 4.1%	4.1–48 cm (mean 13 cm)	F7 2.31%	1–15 cm (mean 4.1 cm)	F7 2.57%	0.3–42.5 cm (mean 3 cm)	F8 2.03%	0.8–20 cm (mean 4.3 cm)	F10 3.28%	0.3–13 cm (mean 2.2 cm)	F9 3.85%	0.1–2.5 cm (mean 0.6 cm)
F6 0.21%	10–13.5 cm (mean 11.8 cm)	F3 1.98%	3–55 cm (mean 11.8 cm)	F10 0.66%	0.8–10 cm (mean 3.5 cm)	F10 0.23%	0.5–5 cm (mean 1.9 cm)	F4 1.63%	2–29 cm (mean 14.1 cm)	F9 1.87%	0.2–4 cm (mean 1.1 cm)	F5 0.79%	0.2–7 cm (mean 3.6 cm)
F5 0.19%	1.8–6.5 cm (mean 4.2 cm)	F9 1.57%	0.2–2.3 cm (mean 0.7 cm)	F9 0.05%	2 cm (mean 2 cm)	F8 0.1%	0.8–3 cm (mean 1.5 cm)	F10 1.11%	0.5–14 cm (mean 3.7 cm)	F4 0.58%	25 cm (mean 25 cm)		
		F1 0.92%	11–22 cm (mean 14.7 cm)			F9 0.02%	0.2–1 cm (mean 0.6 cm)	F9 0.51%	0.3–4.5 cm (mean 1.5 cm)	F5 0.30%	0.4–7.5 cm (mean 2.6 cm)		
								F5 0.12%	0.8–5 cm (mean 3.1 cm)				

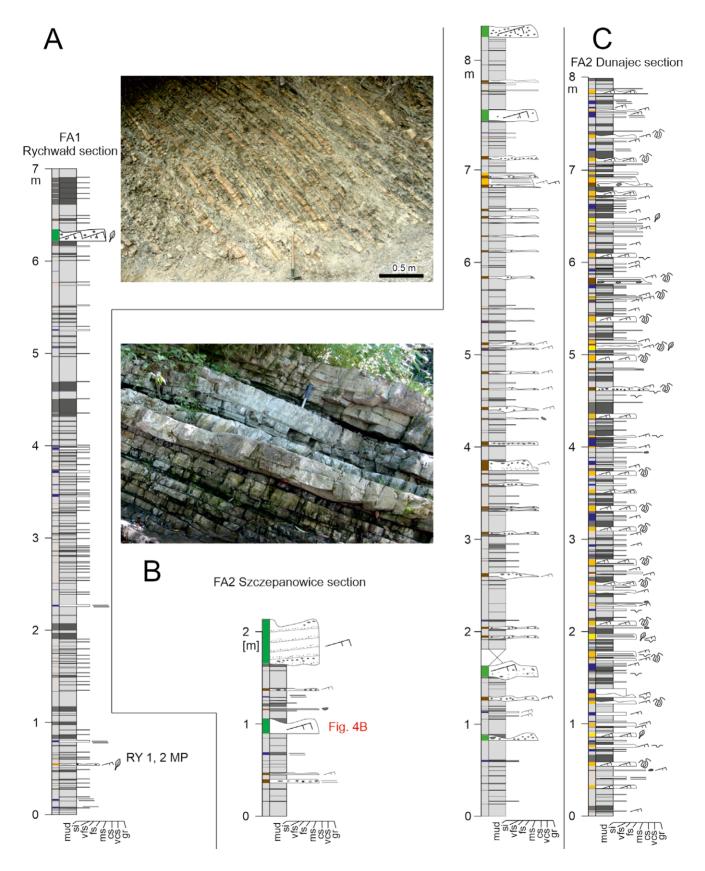| Sandstone bed thicknesses:		Sandstone bed thicknesses:		Sandstone bed thicknesses:		Sandstone bed thicknesses:		Sandstone bed thicknesses:		Sandstone bed thicknesses:		Sandstone bed thicknesses:	
Median	2.8 cm	Median	2.5 cm	Median	52 cm	Median	47.9 cm	Median	14.5 cm	Median	5.2 cm	Median	4 cm
Mean	5.2 cm	Mean	4.2 cm	Mean	66.5 cm	Mean	64.6 cm	Mean	20.1 cm	Mean	8.8 cm	Mean	6.1 cm
Variance	315.6 cm^2	Variance	31.7 cm^2	Variance	2194.2 cm^2	Variance	3305.8 cm^2	Variance	333.2 cm^2	Variance	108 cm^2	Variance	33.1 cm^2
Standard deviation	17.8 cm	Standard deviation	5.6 cm	Standard deviation	46.8 cm	Standard deviation	57.5 cm	Standard deviation	18.3 cm	Standard deviation	10.4 cm	Standard deviation	5.8 cm
Sandstone net/gross	0–21% (mean 9.9%)	Sandstone net/gross	6–28.3% (mean 19.7%)	Sandstone net/gross	71.8–98.9% (mean 85.5%)	Sandstone net/gross	52.5–99.8% (mean 94.2%)	Sandstone net/gross	46.9–93.9% (mean 76.5%)	Sandstone net/gross	43.2–80.2% (mean 59%)	Sandstone net/gross	7.8–41.2% (mean 30.7%)

Fig. 5. Representative sedimentary logs of marlstone-dominated lower-slope and base-of-slope deposits (FA1) and marlstone-dominated lower-slope and base-of-slope bypass zone (FA2). **A.** Marlstone-dominated lower-slope and base-of-slope deposits (FA1) in the Rychwałd section. **B, C.** Marlstone-dominated lower-slope and base-of-slope bypass zone (FA2) in the Szczepanowice and Dunajec sections. For the full legend, see Figure 7.

Interpretation: This facies association represents monotonous sedimentation, dominated by low-density calcareous turbidites. It is now believed that the formation of the marl-rich packages occurred during the final phase of sea-level rise and mainly during the sea-level highstand and early fall, when the accommodation space of the shelf increased and the supply of siliciclastic sediment was reduced (Kędzierski and Leszczyński, 2013). Simultaneously, carbonate material production on the shelf and upper slope was intensified by nutrient delivery from the upwelling (Kędzierski and Leszczyński, 2013). After accommodation space on the margin of the Skole Basin had been exceeded, redeposition of carbonate material was significantly intensified through transfer by turbidity currents basinwards. The appearance of solitary sandstones (especially thick- and very thick-bedded) indicates that siliciclastic deposition did not cease entirely. FA1 is interpreted as being deposited on the lower slope or base-of-slope outside the main sediment pathways during the relative sea-level highstand and carbonate overproduction on the surrounding shelves and upper slope. The overall small thickness of the marlstone beds is perhaps related to the early expansion of flows, which had not been captured by the main pre-existing sediment pathways, such as canyons, slope valleys, or channels, incised into basin slope. Instead, they were spread by turbidity currents over the low-relief basin slope and uniformly covered it. Only in the log of Basowy 1 borehole, the occurrence of marlstone with slump features was reported at a depth of ~1180 m, indicating a slope inclination large enough for at least rare mass-transport events, but overall, turbidity currents predominated. Similar deposits are widely described along the entire northern edge of the Skole Basin, representing the most proximal zone, exposed in the Skole Nappe (e.g., Bromowicz, 1974; Kotlarczyk, 1978, 1988a; Łapcik et al., 2016; Kowalczewska and Gasiński, 2018; Łapcik, 2018, 2019).

Facies association 2 (FA2): Marlstone-dominated lower-slope and base-of-slope bypass zone

Description: This facies assemblage is dominated by fine-grained deposits (sandstone net-to-gross of 6% to 28.3%), with a significantly higher proportion of marlstone (57.7% of facies F8) compared to mudstone (16.1% of facies F7). Sandstone facies amount to 19.7% in total, with their distribution as follows: F2 (9.9%), F5 (4.4%), F6 (4.1%), and F3 (2%). Sandstone beds commonly show convolution and soft-sediment deformation, negative lenticular shapes with erosional bases, bedform-like shapes, and lateral pinch-outs (Fig. 5B, C). The thicknesses of the sandstone beds range from 0.7 to 55 cm (mean 4.2 cm; median 2.5 cm). Very distinctive for FA2 is the proportion of facies F5 and F6, the highest of all of the described FAs. The mean amount of these facies is 8.5% in a particular package, and either facies F5 or F6 may predominate. Heterolithic deposits (F10) and siltstones (F9) account for 4.2% and 1.6%, respectively, but as in the case of FA1, their amount can be underestimated. Even very thin- and thin-bedded siltstone and sandstone contain scattered millimetre-size mud chips. FA2 occurs in packages of 2 to 21.6 m thick (mean

ca. 9.8 m), without significant changes in trends of grain size and bed thickness.

Interpretation: FA2 is closely related to FA1, owing to their similar facies proportions and interfingering, but it is more influenced by the siliciclastic sediment pathways. Despite the lack of a higher proportion of thick-bedded sandstone, the largest amount of lag and bypass deposits (facies F5 and F6) out of all the FAs described supports the interpretation of FA2 as a bypass zone of siliciclastic sediment. The relatively high proportion of dispersed extrabasinal and intrabasinal clasts in facies F1–3, F5 and F6 indicates deposition close to an area of major erosion. This increased intrabasinal erosion may indicate synsedimentary tectonic activity that left the slope out-of-grade. The main dissimilarity between FA2 and the characteristics of the channel-lobe transition zone (e.g., Normark et al., 1979; Kenyon and Millington, 1995; Palanques et al., 1995; Morris et al., 1998; Wynn et al., 2002; Stevenson et al., 2015; Tinterri et al., 2017; Brooks et al., 2018) is that lag deposits of facies F5 and F6, predominate over small-scale scour surfaces and erosional features. This can be explained as 1) the record of the more distal or lateral area of the channel-lobe transition zone from the mouth of the feeder-channel system or 2) the underdeveloped channel-lobe transition zone, where the channel never propagated fully through the zone (Brooks et al., 2018). In the study area, there is no direct link between FA2 and the channel-fill facies; therefore, FA2 most likely represents a different type of bypass zone, compared to the more frequently described channel-lobe transition zone.

The variable development of FA2 may correspond to the complexity of the bypass zone, with adjacent areas of erosion, bypass, deposition, and bottom reworking. Particular logged sections, interpreted as FA2, may represent different parts of the bypass zone, dominated by different transport and depositional processes, thus resulting in a varied arrangement of facies, especially facies F5 and F6. Sedimentation with a significant contribution of lag deposits and convolute lamination is rather characteristic for an area close to a hydraulic jump, e.g., a break-in-slope area (Tinterri et al., 2017).

Facies association 3 (FA3): Channel-fill deposits and channel-lobe transition zone

Description: Facies assemblages of this type occur as sand-rich bodies, ~5.6 to 36.6 m thick (mean ~17.7 m), dominated by sandstone and conglomerate (sandstone net-to-gross from 71.8 to 98.9%) of facies F1 (40.6%), F2 (23.5%) F4 (14.5%) and F3 (6.3%). Beds of sandstone and conglomerate show their highest statistical parameters (mean 66.5 cm; median 52 cm). Facies F11 also accounts for a significant proportion, reaching its maximum in the entire study area (12.2%). The reason why FA3 is less 'sandy' than FA4, but still represents a higher-energy depositional environment, is the occurrence of facies F11, which was included in mud in estimation of the sand-mud ratio. The remaining fine-grained facies, reaching in total up to ~3%, are dominated by facies F7 (2.3%). Sandstones and conglomerates are dominated by graded and ungraded, thick, and very thick beds, which include the coarsest grain sizes in the entire study

area (Fig. 6). Amalgamated beds, erosional bases, grain-size breaks, and dewatering structures are common. These facies assemblages display thinning- and fining-upwards trends, the pattern of which may be affected by irregular occurrences of debrite facies F4 and F11. This facies association was documented in detail only in the Zagórze section.

Interpretation: The highest proportion of coarse-grained sandstone and conglomeratic facies (mostly of facies F1) and debritic deposits of facies F11, together with the highest amount of erosional features, bed amalgamation, and a fining-and thinning-upward trend supports the interpretation of it as a submarine channel fill (cf. Mutti and Normark, 1987; Gardner *et al.*, 2003; Mayall *et al.*, 2006; Hubbard *et al.*, 2008, 2014, 2020; Janocko *et al.*, 2013; Covault *et al.*, 2016; Baas *et al.*, 2021). However, the strong aggradational trend without variation in facies association over ~60 m of the Zagórze section, and its further upward transition into the lobe-axis FA4, provide an additional premise to consider. FA3 could represent a more complex environment, bearing a characteristic of both channel-fill deposits (perhaps of a multistorey nature) as well as the channel-lobe transition zone (Wynn *et al.*, 2002; Stevenson *et al.*, 2015; Brooks *et al.*, 2018) in one facies association, which are difficult to separate in the studied log. The true thickness of sandstone beds remains unknown, owing to common amalgamation and erosion, which in turn affects the results of the statistical characteristic of FA3 with decreased values of median, mean, variance and standard deviation of sandstone bed thickness (Tab. 1). Studies in the excellently exposed deep-water systems showed that channel fills can show a more complex internal structure than that described here and only large-scale scour features are obvious evidence of their true position. Therefore, the presented proportion of FA3 (reported only in the Korzenna, Zagórze, and Lichwin sections) in the study area may be higher at the expense of the sand-rich facies associations FA4 described below, owing to the poor exposure of diagnostic large-scale scour features. The general statistical characteristics of submarine-channel fill in the study area make it comparable to the facies associations of a channel-fill, described in the more eastern part of the Skole Basin (Łapcik, 2018, 2019).

Facies association 4 (FA4): Lobe-axis deposits

Description: This facies association is characterised by packages 3–9.3 m thick with the highest mean contribution of sandstone (sandstone net-to-gross from 52.5% to 99.8%, mean 94.2%). The proportions of sandstone by facies are as follows: F1 (73.7%), F2 (10.3%), F4 (5.6%), and F3 (4.6%). The sandstone beds are mostly tabular, with common dewatering structures. In contrast to the FA3 amalgamated beds, erosional features are less abundant and grain size decreases significantly to predominantly medium- and fine-grained sand (Fig. 7). However, the overall mean thickness (64.6 cm) and median thickness (47.9 cm) of the sandstone beds remain similar. Fine-grained facies (~3% in total) are mostly represented by facies F7 (2.6%). This facies association is widespread in the numerous sections of the study area.

Interpretation: This facies association is characterised by thick- and very thick-bedded sandstones, which are more fine-grained than FA3. A high proportion of tabular beds, dominated by F1, together with a lower amount of amalgamation, erosion, and grain size breaks, implies interpretation as a relatively proximal depositional environment of high energy, such as the axial part of a depositional lobe (cf. Mutti and Normark 1987; Pickering *et al.*, 1995; Deptuck *et al.*, 2008; Prélat *et al.*, 2009; Bernhardt *et al.*, 2011; Prélat and Hodgson, 2013; Grundvåg *et al.*, 2014; Marini *et al.*, 2015; Łapcik 2017, 2019; Hansen *et al.*, 2019; Baas *et al.*, 2021).

Facies association 5 (FA5): Lobe-off-axis deposits

Description: This facies assemblage shows a gradual decrease in the proportion of sandstone (sandstone net-to-gross 46.9% to 93.9%) and in bed thicknesses (mean 20.1 cm; median 14.5 cm), compared to FA4 (Figs 7, 8). The FA5 packages are 1.7 to 19.5 m thick (mean ~6 m) and show a further shift of the facies distribution to the dominance of deposits, generated by the relatively lower-energy currents of facies F2 (45.2%) and F3 (13%) over high-density turbidity currents F1 (16.5%). Sandy debrites F4 (1.6%) remain marginal, but HEBs are present. The general proportion of fine-grained facies increases, with the highest change in facies F7 (10.8%).

Interpretation: Gradual thinning of sandstone beds and increase in finer-grained facies support the interpretation of this facies assemblages as a lateral or downflow equivalent of FA4 and, therefore, sediments of depositional lobe-off-axis (cf. Mutti and Normark 1987; Deptuck *et al.*, 2008; Prélat *et al.*, 2009; Bernhardt *et al.*, 2011; Prélat and Hodgson, 2013; Grundvåg *et al.*, 2014; Łapcik, 2017, 2019; Spychala *et al.*, 2017; Hansen *et al.*, 2019; Baas *et al.*, 2021).

Facies association 6 (FA6): Lobe-fringe deposits

Description: This facies association reflects a further decrease in the thickness and proportion of sandstone beds (sandstone net-to-gross 43.2–80.2% with mean 59%) of the sandy facies (Figs 7, 8). FA6 is organised into packages 0.8–5.7 m thick (mean ~3.1 m), where there are mainly thin beds (mean 8.8 cm; median 5.2 cm). Facies F2 (36.1%) remains the most common, and the amount of facies F3 (14.2%) exceeds that of facies F1 (8.4 %). HEBs occur, but facies F4 (0.6%) is very rare. A high increase in fine-grained facies is noticeable, with the predominance of facies F7 (30.9%).

Interpretation: The decrease in the mean proportion of the sandstone net-to-gross from 76.5% in FA5 to 59% in FA6, together with the finning and thinning of beds, reflects a further shift towards the distal area of the depositional lobe. FA6 is interpreted as the deposits of the lobe fringe (e.g., Prélat *et al.*, 2009; Grundvåg *et al.*, 2014; Łapcik, 2017, 2019; Spychala *et al.*, 2017; Hansen *et al.*, 2019).

Facies association 7 (FA7): Interlobe deposits/lobe-distal-fringe deposits

Description: This facies association is characterised by the highest proportion of fine-grained facies (Fig. 8), with simultaneous domination of mudstone facies F7 (29.7%)
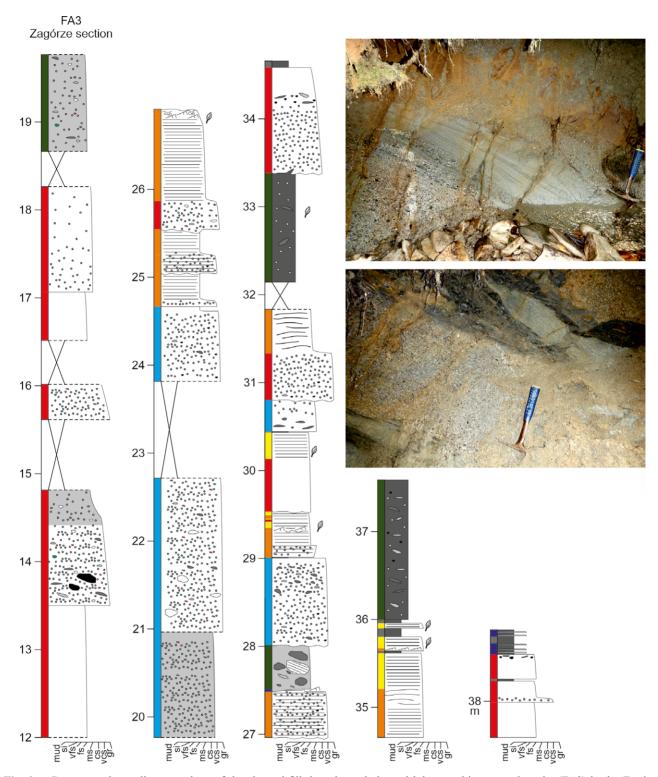
Fig. 6. Representative sedimentary logs of the channel-fill deposits and channel-lobe transition zone deposits (FA3) in the Zagórze section. For the full legend see Figure 7.

over marlstone facies F8 (27.3%). The packages of this facies assemblage are 0.8–5.5 m thick (mean 2.9 m). FA7 is poor in predominantly thin-bedded (mean 6.1 cm; median 4 cm) sandstone facies (sandstone net-to-gross 7.8–41.2% with mean 30.7%), which are represented almost entirely by facies F2 (22.7%) and F3 (7.2%). Still, some rare beds of sandstone, up to 30 cm, are randomly distributed in the logs.

Heterolithic deposits (F10 8.5%) and siltstone (F9 3.9%) reach their maximum in FA7.

Interpretation: This facies association represents the sedimentary environment with the lowest energy in the study area, dominated by siliciclastic deposition. The predominance of the fine-grained facies implies the most distal setting or at least the least energetic sedimentary environment,

Fig. 7. Representative sedimentary logs of lobe-axis deposits (FA4), lobe-off-axis deposits (FA5) and lobe-fringe deposits (FA6) in the Janowice section. JAN 1–28, 29 dark and light represent beds sampled for grain-size analysis (Supplementary Material 1, Table S1).

by comparison with the previously described facies. FA7 is interpreted as lobe-distal-fringe or interlobe deposits, reached by mainly low-density turbidity currents (e.g., Prélat *et al.*, 2009; Grundvåg *et al.*, 2014; Łapcik, 2017, 2019; Spychala *et al.*, 2017; Boulesteix *et al.*, 2020).

DISCUSSION

Evolution of the depositional system in the western part of the Skole Basin

The stratigraphic grouping of sedimentary logs from the southern (Fig. 12) and northern areas (Figs 13, 14) into time intervals was based primarily on the spatial distribution of similar facies associations and the lateral extension of four characteristic sand bodies (SB1–4). These were the main tools for correlation between particular sections and between the southern and northern areas, represented by different thrust sheets (Fig. 15). Additionally, dating of calcareous nannoplankton and foraminifers and previous studies of this area (Marciniec *et al.*, 2006, 2014) were considered. However, some disagreements in micropalaeontological dating with previous studies occurred (see Supplementary Material, Table S2; cf. Marciniec *et al.*, 2006, 2014). Four stages (S1–4) of the late Cretaceous–Paleocene evolution of the western part of the Skole Basin were distinguished, each starting with a particular SB, except for stage S1, containing SB1 in the middle of the sedimentary succession (Fig. 16). The entire sedimentary succession was compared with the lithostratigraphic chart of the Skole Basin (Kotlarczyk, 1978, 1988a; Malata, 1996; Fig. 2). The evolutionary stages of the study area are described and interpreted below.

Stage 1 (S1): Early Campanian

The oldest deposits of the Ropianka Fm in the study area are dated as early Campanian to early late Campanian and represent stage S1 (Figs 9, 13), which exceptionally begins with marlstone-dominated sedimentation instead of a sand body, as in the later stages. In the southern area (Lubinka and Dunajec sections), an episode of intense siliciclastic sedimentation was distinguished (SB1), which led to the subdivision of stage S1 into three substages (S1a, S1b, S1c; Fig. 9). In the southern area (Dunajec, Lubinka, Pleśna and Rychwałd sections), substage S1a is represented by marlstone-dominated sedimentation, with sparse thick and very-thick bedded sandstone (FA1) limited to the Dunajec section (log interval 11–54 m; Fig. 9). In the lowermost part of the Dunajec section (log interval 0–9 m; Fig. 9), marlstone-dominated deposits with dune bedforms and lag deposits (FA2) indicate the location of the sediment bypass zone with palaeotransport towards the E along the basin axis. This area was affected by sustained turbulent flows, which reworked the sand-starved substratum into dune-scale bedforms (cf. facies F5 in Tinterri *et al.*, 2017). In the Dunajec and Lubinka sections, above the marly deposits (FA1) of substage S1a, the beginning of the second substage S1b is represented by an SB1, tens of metres thick (Fig. 9). Only the Lubinka section was exposed well enough for detailed logging of this substage. The Lubinka sand-rich section starts with the
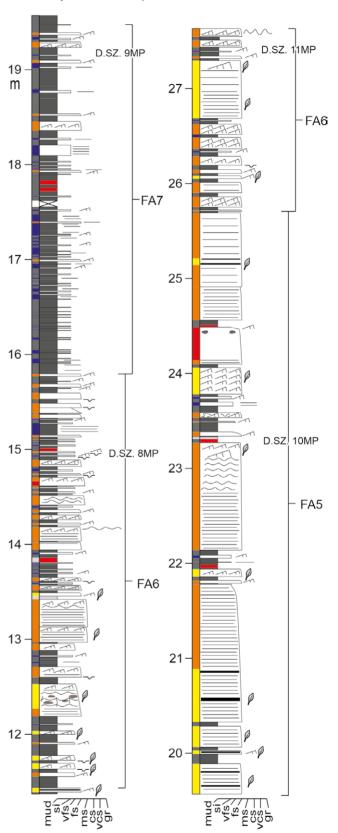

Fig. 8. Representative sedimentary logs of lobe-off-axis deposits (FA5), lobe-fringe deposits (FA6), and interlobe / lobe-distal-fringe deposits (FA7) in the Dąbrówka Szczepanowska section. D.SZ 8–11MP mark place of the micropalaeontological sample collection. For the full legend see Figure 7.
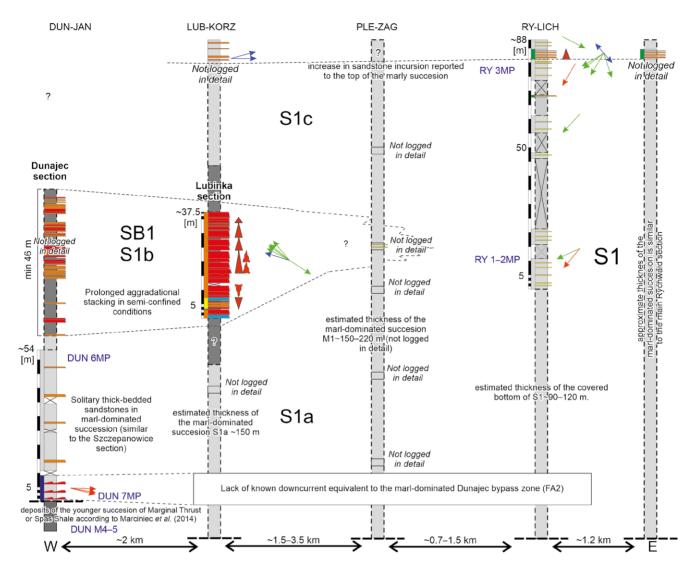
Fig. 9. Simplified sedimentary logs of the Janowice-Lichwin Syncline, stage S1. Blue labels mark the approximate position of the micropalaeontological samples. An additional explanation is given in Figure 10. Abbreviations: DUN-JAN (Dunajec-Janowice sections); LUB-KORZ (Lubinka-Korzenna sections); PLE-ZAG (Pleśna-Zagórze sections); RY-LICH (Rychwałd-Lichwin sections). Note that only sections with distinguished facies associations were logged in detail. Logs 'not logged in detail' are synthetic representations of observed outcrops and map estimates. Owing to the small number of palaeotransport direction measurements in particular outcrops, data are presented as arrows instead of the typical rose diagram.

thickening-upward deposits of a prograding depositional lobe, formed in a lobe-axis setting (FA4; log interval 0–3 m; Fig. 9), terminated with abrupt abandonment, recorded as thin muddy interlobe deposits (log interval 3–3.3 m; Fig. 9). Up the section, the occurrence of HEBs and banded sandstone is related to a period of development of the lobe-off-axial setting (FA5; log interval 3.3–6.8 m; Fig. 9), which initiated the prolonged aggradation of the depositional lobe. For the remaining portion of the section (log interval 6.8–38 m; Fig. 9), the lobe-axis (FA4) setting occurs without important signs of lobe compensational stacking or shifting of the depositional environment, but with the disappearance of the HEBs up the section. Changes in bed thickness indicate the distinction of 5 or 6 lobe elements (*sensu* Prélat *et al.*, 2009) in the lobe-axis setting (Fig. 9). Palaeotransport data are sparse and show directions towards the NW, indicating the first record of southern source (Węglówka Ridge)

activity (Figs 9, 16). Superimposed marl-dominated deposits (FA1) belong to substage S1c and are mostly covered in the Lubinka area (Fig. 9). Their uppermost part is exposed closer to the Korzenna area in the Lubinka Stream (Fig. 15). Farther to the E, in the Rychwałd section, there are no signs of substage S1b (Figs 9, 15). Instead, sand-starved marly sedimentation (FA1) remains uninterrupted without significant changes throughout the entire stage S1, and palaeotransport is towards the SE, with a source in the northern margin of the Skole Basin (Fig. 9). The increasing influence of the siliciclastic source is recorded in the repeated alternation of the marlstone-dominated lower-slope and base-of-slope deposits (FA1) and lobe-distal-fringe deposits (FA7), reported from the Lubinka (not logged in detail) and Rychwałd (log interval 67–85 m; Fig. 9) sections, with a decrease in the marl-to-mud ratio. During the substage S1c, the area of Lubinka again shows axial palaeotransport
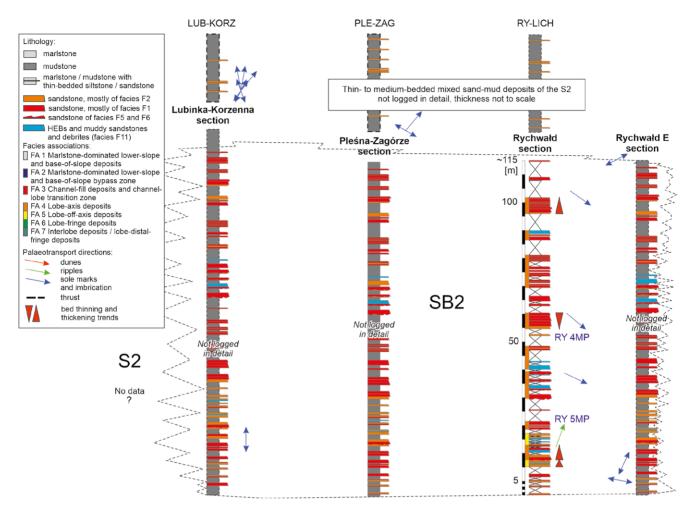
Fig. 10. Simplified sedimentary logs of the Janowice-Lichwin Syncline, stage S2. Blue labels mark the approximate positions of the micropalaeontological samples. Additional explanation is given in the description of Figure 9.

and the Rychwałd section shows palaeotransport towards the SW, S and SE (Fig. 9).

The northern area records more monotonous marlstone-dominated sedimentation throughout stage S1 (Fig. 13). The thickness of the best exposed sedimentary succession in Szczepanowice, dominated by deposits of FA1 with sparse thick- and very thick-bedded sandstones, is estimated at ~180 m in total (Fig. 13). This sedimentary succession is a northern equivalent of the three substages (S1a–c), described in the southern area (Figs 9, 13, 16). The absence of an unambiguous equivalent of the SB1 deposits in the Szczepanowice section makes it similar to the Rychwałd section (Figs 9, 13). According to the general sedimentary changes during the stage S1, there is an increasing influence of siliciclastic sedimentation and repeated incursions of lobe-distal-fringe deposits (FA7) in the upper part of the Szczepanowice section. The siliciclastic deposits in the Szczepanowice and Dąbrówka Szczepanowska sections mainly show palaeotransport directions toward the S, SE and E (Fig. 13). In the middle and upper parts of the Szczepanowice section, some palaeotransport directions are toward the NW and SE (Fig. 13).

Interpretation: Clast-rich deposits with dune bedforms (facies F6) of the Dunajec bypass zone (FA2; substage S1a in Fig. 9) are evidence of the upcurrent erosion of the muddy

substratum and significant sediment bypass (cf. Stevenson *et al.*, 2014; Tinterri *et al.*, 2017). However, no downcurrent siliciclastic equivalent to this bypass zone was reported in the outcrops to the east, which in turn points to the basinward transfer of siliciclastic sediment at a minimum distance of ~8 km (Figs 9, 15, 16). Near the Dunajec area, sediment gravity flows reached a hydraulic jump, eroding the muddy substratum, and left part of their coarsest fractions, which transformed them into predominantly non-depositional flows over a distance of at least several kilometres.

The rare thick- and very-thick bedded sandstones, reported within FA1 at the Dunajec (log interval ~14–47 m; Figs 9, 16) and Szczepanowice (log interval ~90–100 m; Figs 13, 16) sections during substage S1a, are limited to the most marginal part of the study area. They may represent small intraslope sandy lobes, which captured some of the sediment in local ponds, perhaps inherited after periods of increased erosion in the sediment bypass zones or small slump scars in the northern basin slope. The concentration of siliciclastic deposits in these solitary beds indicates temporal pulses of increased siliciclastic supply to the basin. Different numbers of thick beds and different thicknesses of marly intervals between them prevent their corelation between the Dunajec and Szczepanowice sections (Figs 9, 13) and imply a relatively small lateral extent of these sandy
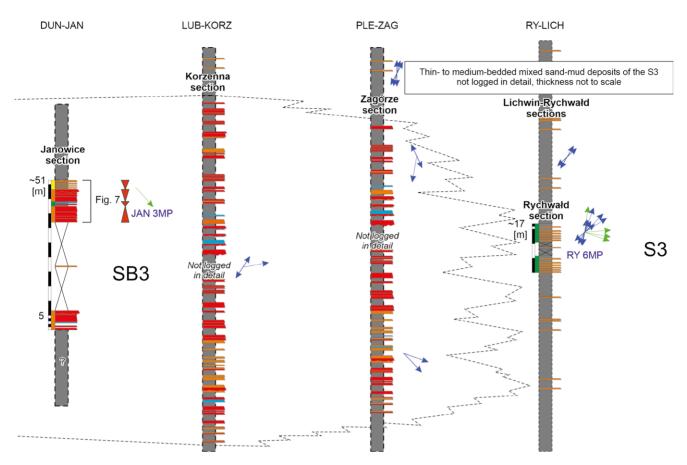
Fig. 11. Simplified sedimentary logs of the Janowice-Lichwin Syncline, stage S3. Blue labels mark the approximate positions of the micropalaeontological samples. Additional explanation is given in the descriptions of Figures 9 and 10.

bodies (Fig. 16). An alternative interpretation of the thick-bedded sandstones indicates their formation as the more distal and finer-grained deposits of flows, which in the proximal area were responsible for the formation of the dune deposits of facies F6, e.g., in the Dunajec section. In such a case, the occurrence of thick-bedded sandstones above the dune deposits in the Dunajec section can be explained by the retreat of the source for >8 km, resulting in retrogradation of the siliciclastic system.

Development of the small fan (SB1) in the southern area during substage S1b (Dunajec and Lubinka sections; Figs 9, 14) marks the activation of the Węglówka Ridge as a source (Fig. 16). It is more likely that this was triggered by tectonic impulse, rather than by eustatic sea-level change, due to the uninterrupted marl sedimentation in the Rychwałd and Sczepanowice sections through stage S1 (Figs 9, 13) and the change in the equilibrium profile that resulted in the generation of HEBs (cf. Pszonka et al., 2023 and references therein). The lack of evidence for propagation of the Lubinka-Dunajec fan eastward and the NW palaeotransport directions are in contrast to the SW palaeotransport directions in the Rychwałd section (Fig. 9). This can be explained by the formation of temporary confinement, provided by the hypothetical tectonic elevation, originating from the same tectonic trigger, which activated the Węglówka Ridge (Fig. 16). This transverse tectonic obstacle could have separated the western and eastern parts of the basin and forced

the propagation of sediment gravity flows to the NW (Tinterri et al., 2020, 2022). The confinement also could account for the lack of a clear compensational stacking pattern and a strong aggradation trend of the depositional lobe in the Lubinka section (Fig. 9). A transverse obstacle also could explain the appearance of a northward palaeotransport direction in the middle part of the Szczepanowice section (Fig. 13) as a sign of overspill of the dilute flows, which were less affected by the confinement and/or inclination of the northern slope. Before the beginning of stage S2, the seafloor was already healed and transport along the axis of the basin was restored, at least in the area of the Lubinka section (Figs 9, 16). Increasing siliciclastic supply during substage S1c heralded sea-level fall and the beginning of progradation of the turbidite complexes (Fig. 16).

Micropalaeontological dating, lithological characteristics and stratigraphic position of the described marly deposits fit well the lithostratigraphic chart of the Skole Basin (Fig. 2) and allow them to be distinguished as the western equivalent of the Kropivnik Fucoid Marl (lower Campanian–lower upper Campanian). The early Campanian stage S1 is interpreted as the progradation of slope and base-of-slope deposits, dominated by redeposited carbonates during the final phase of sea-level rise and mainly sea-level highstand and early fall (Kędzierski and Leszczyński, 2013) with episodes of siliciclastic sediment incursions and bypass, caused by small-scale sea-level changes and/or tectonic activity.
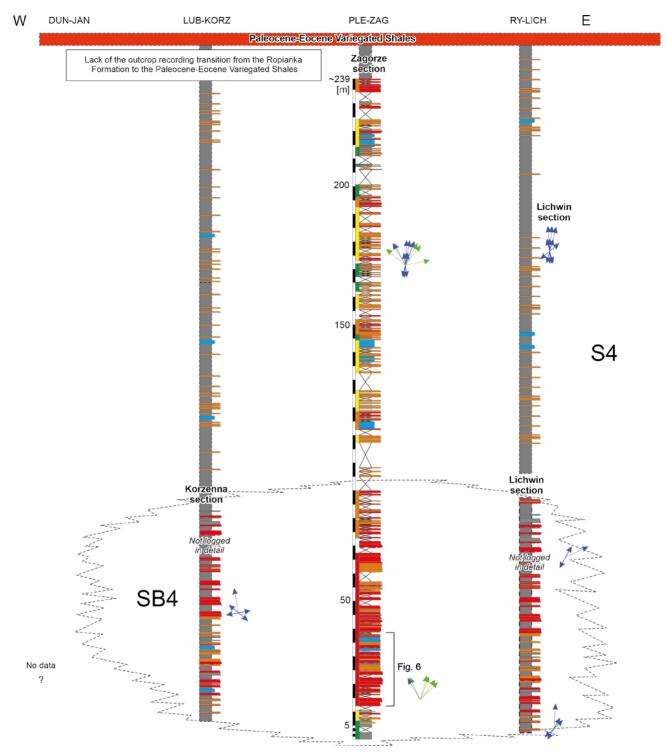
Fig. 12. Simplified sedimentary logs of the Janowice-Lichwin Syncline, stage S4. Blue labels mark the approximate positions of the micropalaeontological samples. Additional explanation is given in the descriptions of Figures 9 and 10.

Stage 2 (S2): late Campanian

During the late Campanian, sedimentation switched from carbonate- to siliciclastic-dominated, resulting in the development of a sedimentary succession, a few hundred metres thick. This change already was begun during the early Campanian (S1c) and recorded as an increase in the supply of siliciclastic deposits up the Szczepanowice and Rychwałd sections (Figs 9, 13). Stage S2 represents a full spectrum of depositional environments from the axial zone of depositional lobes (FA4) and distributary-channel fill (FA3) to interlobe sediments (FA7), concentrated in SB2 and mostly thin- to medium-bedded succession above, for which lateral tracking and correlation are difficult (Fig. 15). Palaeotransport directions during stage S2 indicate the fan-shaped distribution of the deposits and the propagation of the channel-lobe complex, mostly longitudinally relative to the basin margins, in accordance with the general inclination of the basin floor (Fig. 16; cf. Książkiewicz, 1962; Bromowicz, 1974).
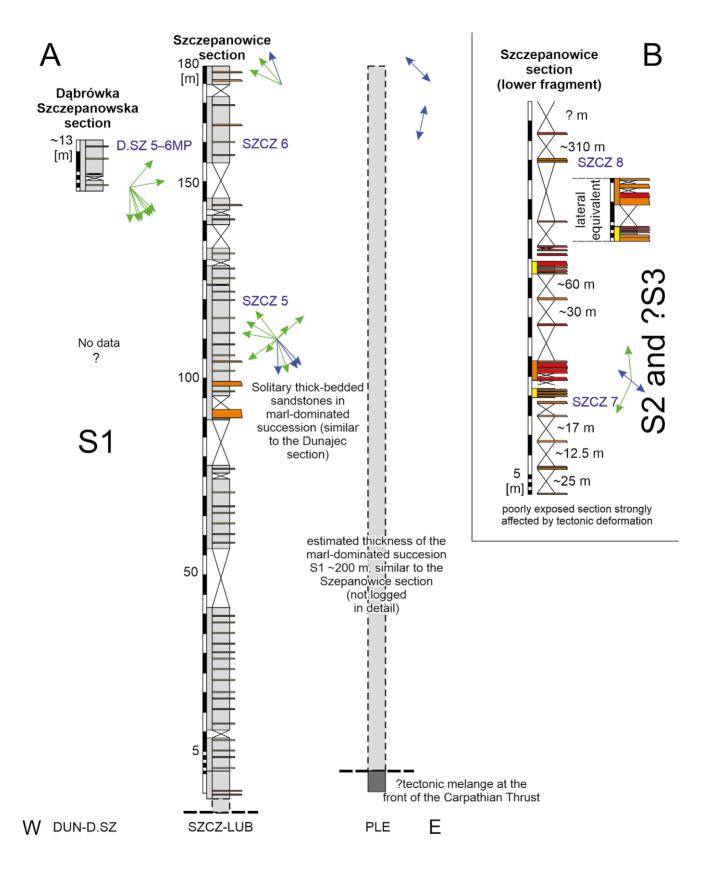
Fig. 13. Simplified sedimentary logs of the Marginal Anticline. **A.** Stage S1. **B.** Stage S2. Blue labels mark the approximate positions of the micropalaeontological samples. Abbreviations: DUN-D.SZ (Dunajec-Dąbrówka Szczepanowska sections); SZCZ-LUB (Szczepanowice-Lubinka sections); PLE (Pleśna section). Additional explanation is given in the descriptions of Figures 9 and 10.
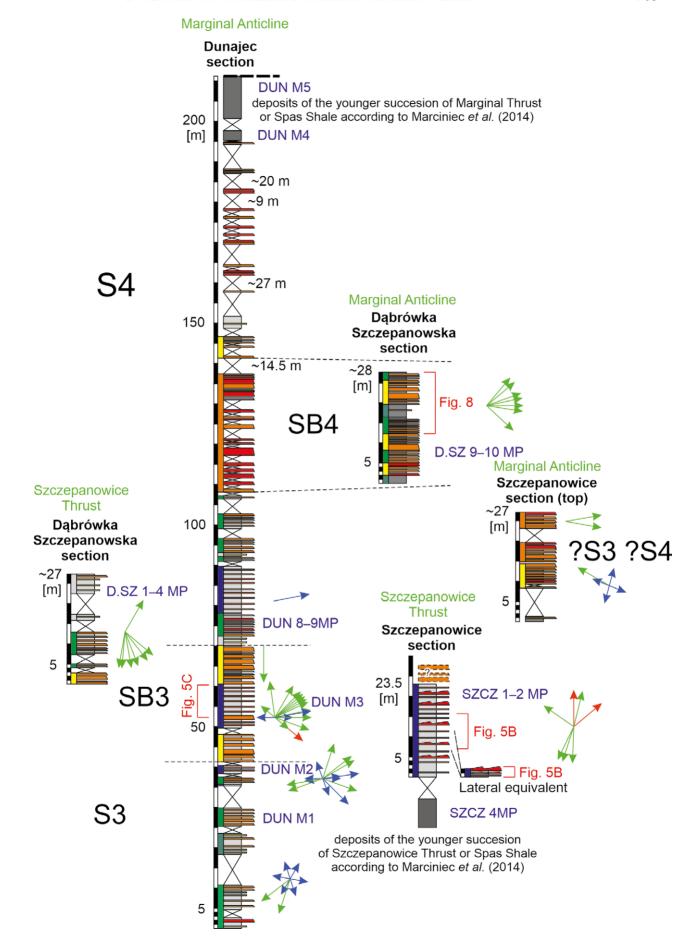
Fig. 14.   Simplified sedimentary logs of the Marginal Anticline and Szczepanowice Thrust, stages S3 and S4. Blue labels mark the approximate positions of the micropalaeontological samples. Additional explanation is given in the descriptions of Figures 9 and 10.
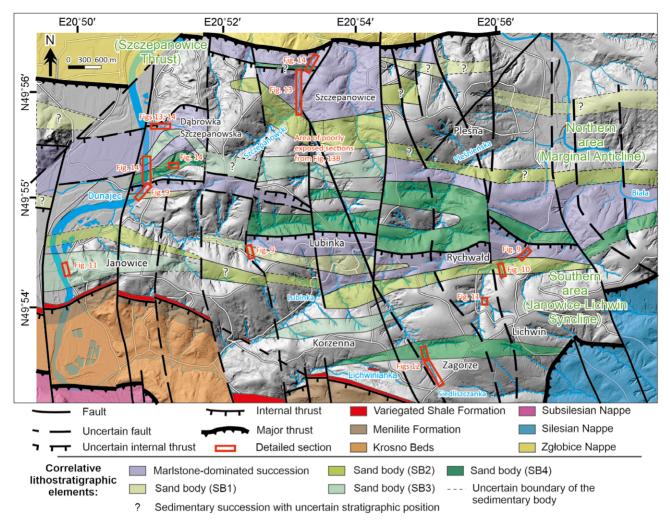
Fig. 15. Facies map of the study area with an overlay of a hillshade terrain model (https://baza.pgi.gov.pl/cbdg/geoportal) and distinguished sandy bodies (SB1–4) and marl-dominated facies. Geology and tectonics are based on Marciniec *et al.* (2006, 2014), with modifications based on field observations.

During stage S2, the southern area shows the appearance of a well-developed sand-rich succession (SB2), documented in the Rychwałd section, but extending eastward at least to the Lubinka-Korzenna area (Figs 10, 16). These sediments of a depositional-lobe complex are at least 115 m thick and dominated by a lobe-axis setting, with a subordinate proportion of deposits forming a distributary channel-fill, incised in the depositional lobe and lobe-off-axis settings (Fig. 10). The Rychwałd section contains structureless muddy sandstones of facies F4, the proportion of which decreases up the section. The Rychwałd succession records the maximum progradation of the channel-lobe complex in the study area during the late Campanian, with sparse palaeotransport directions to the SE and NE (Figs 10, 15). Up the Rychwałd section above SB2, the deposits are dominated by the more distal settings of FA5, FA6, and FA7, but without significant cessation of the influence of the siliciclastic source.

Similar facies associations occur in the northern area in the Szczepanowice section and in section E of it, where poor exposure and tectonic deformation permit only general insight into the depositional environment (Fig. 13). This area is mostly represented by the deposits of shifting sub-environments of the depositional lobe FA4, FA5, FA6, and FA7,

probably owing to compensational stacking. Sparse measurements show a wide distribution of palaeotransport directions, which did not allow major sediment pathways to be distinguished in the area.

Interpretation: A significantly increased sand supply from the beginning of stage S2 resulted in a larger volume of sediment gravity flows and a concentration of sandy deposits in SB2, which is far more extensive than SB1 (Figs 10, 15). The expected cause of the supply increase is the development of a shelf-edge delta to the NW of the Skole Basin margin as a result of sea-level fall. Moreover, a change in the equilibrium profile is recorded in the appearance of structureless muddy sandstone of facies F4 (including divisions H3 of HEBs), interpreted as the product of intensified erosion of the muddy substratum up-dip and flow transformation, due to erosional bulking (cf. Haughton *et al.*, 2009). Up SB2, the frequency of facies F4 decreases, indicating gradual slope levelling and decreasing erosion (Fig. 10).

In an unconfined setting, it might be expected that the development of the depositional lobe complex was controlled by the constantly changing topography of the seafloor by build-up of the depositional lobe and/or its graduall
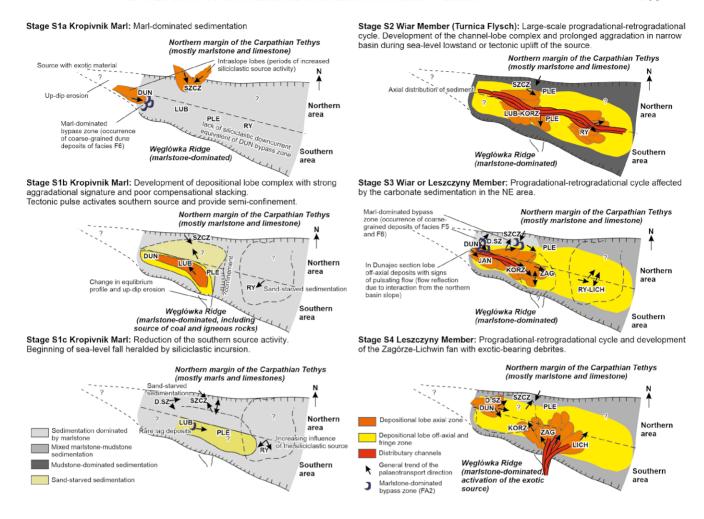
Fig. 16. Four evolutionary stages of the Ropianka Fm south of Tarnów during the Campanian–Maastrichtian.

lateral migration. In such a depositional environment, sediment gravity flows are switching between local topographic depressions in a compensational stacking pattern and/or abruptly shift, owing to updip avulsion of a distributary channel. The sand-rich part of the Rychwałd section (SB2; Fig. 10) is less exposed than the Słonne section, located further to the E of the Skole Basin (cf. Łapcik, 2017). In the Słonne area, the depositional lobe complex was formed in unconfined conditions with enough accommodation space for full development of a compensational stacking pattern, due to lateral migration of the facies association, which is recorded in a wide spectrum of depositional lobe environments in ~140-m-thick log (Łapcik, 2017). In the less exposed, ~115-m -thick Rychwałd section (SB2 in Fig. 10), sediments of the depositional lobe-axis (FA4) predominate with only rare occurrences of succesions interpreted as the depositional lobe-off-axis (FA5). This argument supports interpretation of Rychwałd section development (SB2 in Fig. 10) in a more aggradational stacking pattern, similar to that of the Lubinka section (SB1 in Fig. 9). On the other hand, interlobe and depositional lobe-fringe facies associations are missing and it is unknown what type of depositional environment is recorded in the covered parts of the Rychwałd section (Fig. 10). The thicknesses of gaps in the Rychwałd section are comparable with the thickness of changing subenvironments in the lobe-complex in the

eastern part of the Ropianka Fm (cf. Łapcik, 2017, 2019). Already during substage S1b, the distribution of facies associations FA4 and FA5 showed the limited spatial extension of the strongly aggradational Lubinka depositional lobe (SB1, Fig. 9). Therefore, the author expects that at least the largest-volume flows could have been affected by the limited size of the Skole Basin during stage S2, preventing their free expansion on the local basin floor. This also would have led to the limited possibility of lateral migration or compensational stacking of the depositional lobe sub-environments in the study area. On the basis of the restored cross-section, the width of the Skole Basin in its eastern part was postulated to be ~140 km (Gągała *et al.*, 2012). On the basis of this estimate and a significant reduction in the outcrop width of the Skole Nappe to the west, the author expects that in the study area the basin originally should have been narrower, perhaps not exceeding 50 km or even less. The estimated width of the western part of the Skole Basin could have affected at least the largest sediment gravity flows, resulting in their partial confinement. The bipartite character of stage S2 with SB2 at the base (Figs 10, 13) and the medium- to thin-bedded mixed mud-sand deposits at the top is interpreted as a major progradational-retrogradational cycle of the channel-lobe complex (Fig. 16). The upper fragment of stage S2, represented by the sedimentary succession between the

outcrops of SB2 and SB3 (Figs 10, 13), reflects a relatively abrupt bulk retreat of the turbidite system and shifts towards the facies association, linked with a lower fan setting.

On the basis of micropalaeontological dating, lithological characteristics, and stratigraphic position, the deposits of stage S2 are interpreted as Turnica Flysch, being a part of the Wiar Mbr (Fig. 2; Kotlarczyk, 1978; Malata, 1996). The general shift of sedimentation from carbonate-dominated to siliciclastic-dominated correlates with the beginning of the global sea-level fall, which began during the late Campanian (Haq, 2014), and may have affected the Skole Basin as well, for example, by allowing deltaic source progradation and reducing carbonate production on the shelf (Kędzierski and Leszczyński, 2013; Łapcik, 2019). It is possible that the formation of these deposits of stage S2 was coeval with the development of the Słonne depositional-lobe-complex. The general progradational-retrogradational signature, without significant influence of the carbonate source during stage S2, may represent small-scale sea-level fluctuation.

Stage 3 (S3): early to late Maastrichtian

During stage S3, the distribution of facies associations shows the characteristics of both previous stages. In the western part of the southern area (Janowice, Korzenna, and Zagórze sections), SB3 marks the base of stage S3 (Figs 11, 15). The Janowice section (SB3) contains deposits of the lobe-axis (FA4), the lobe-off-axis (FA5) and the lobe-fringe (FA6) with banded sandstone (F3) and subordinate contribution of HEBs (Fig. 7, 11). In the southern area, as in stage S2, above the sandy body (SB3) sedimentary successionis mostly are represented by muddy sedimentation with alternation of thin- to medium-bedded sandstone. However, stage S3 contains mixed sand-mud-marl packages, though less pronounced than during stage S1. Palaeotransport data indicate E and SE directions in SB3 and additionally N-S in the upper part of the mixed sand-mud interval (Zagórze and Lichwin-Rychwałd sections in Fig. 11). Farther to the E in the Rychwałd and Lichwin sections, fine-grained deposits with an alternation of marlstone represent the entire stage S3 without signs of SB3 and the palaeotransport directions towards the E, NE and N (Figs 11, 15).

In the northern area, the Dunajec and Dąbrówka Szczepanowska sections reflect the alternation of marlstone-dominated deposits with the influence of the siliciclastic source and repeated marlstone-dominated deposits with lag deposits (Fig. 14). In the lower part of the Dunajec section (log interval 0–36 m in Fig. 14), the thin- to medium-bedded deposits rarely alternates with coarse-grained sandstone and granule conglomerate. Noticeably, these deposits contain a high proportion of marlstone, indicating the simultaneous activity of the siliciclastic and carbonate sources. A lateral equivalent of these deposits was logged in the Dąbrówka Szczepanowska section (Figs 14, 15). Up the Dunajec section (log interval ~36–70 m in Fig. 14), the facies association shifts to the alternation of a marlstone-dominated setting with sediment bypass (FA2) and lobe-off-axis desposits (FA5) in a stratigraphic position corresponding to SB3 (Figs 14, 15). Thicker sandstone beds

contain a significant proportion of banded sandstone (facies F3), frequently with a complex internal structure, amalgamation, and repeating planar-parallel and cross-laminated intervals, sometimes indicating changing transport directions. In the log interval between 70–90 m (Fig 14), packages of facies association FA5 are replaced with depositional lobe-fringe (FA6) and marlstone-dominated lower-slope and base-of-slope deposits (FA1) with the last interval of FA2. Ultimately up the section, a depositional lobe-fringe (FA6) setting predominates (log interval 90–107 m in Fig. 14). Palaeotransport data in the Dunajec section show a fan-shaped distribution of directions, predominantly to the NE, E and SE (Fig. 14). In the Szczepanowice section, deposits similar to the Dunajec intervals of FA2 were reported (Fig. 14). Here, they are located close to the margin of the Carpathian Thrust in the Szczepanowice Thrust Sheet and superposed by a sandy interval (?SB3), deduced from the very poor exposures of sandstone beds (Fig. 14). In the Szczepanowice section, palaeotransport measurements show mostly N and S directions (Fig. 14). The Szczepanowice section, located in the Marginal Anticline, is affected by tectonic deformation and is poorly exposed, which obscures the picture of basin development. Sand-rich intervals with the signatures of the depositional lobe-axis (FA4) and off-axis (FA5) settings were identified (Fig. 14). However, in some cases, their stratigraphic position and interpretation as SB2 or SB3 remain uncertain (Fig. 15).

Interpretation: Deposits of stage S3 represent another major progradational-retrogradational cycle, but this time with the simultaneous influence of the carbonate source (Fig. 16). Marly facies associations are less widespread than during stage S1 and are more diluted by accompanying siliciclastic sedimentation (Figs 11, 14, 16). Compared to stage S2, progradation of the lobe complex is limited to the western part of the basin and fully replaced by distal environments to the E, in the Rychwałd and Lichwin sections (Figs 11, 14, 16). On the basis of the small distance between the Dunajec, Dąbrówka Szczepanowska and Janowice sections (contemporary distance ~3 km), it is likely that all sections represent the same channel-lobe complex, with the lobe off-axial (FA5) and fringe (FA6) deposits in the Dunajec and Dąbrówka Szczepanowska additionally affected by the progradation of the carbonate sedimentation, with supply from the northern margin of the basin (Figs 11, 14–16). The appearance of complex beds, with amalgamation and repetition of planar-parallel lamination and cross-lamination with changing current directions in sand rich intervals of the Dunajec section (SB3 in Fig. 14), is evidence of the deflection of sediment gravity flows, due to interaction with the northern basin margin or other topographic obstacles (e.g., Muzzi Magalhaes and Tinterri, 2010; Tinterri and Tagliaferri, 2015; Bell et al., 2018; Siwek et al., 2023). Such features are reported only in thick-bedded sandstones, deposited by flows with enough volume to interact with the basin topography. In the Dunajec section, there is a noticeably high amount of convolute lamination, which also is postulated to be one of the lines of evidence for interaction between flow and the local basin topography (Tinterri et al., 2016, 2022). Some of the palaeotransport directions toward the N or with a N–S trend leave uncertainty

about the activity of the southern source (Węglówka Ridge) at that time.

It is unclear if stage S3 represents part of the Wiar Mbr or the Leszczyny Mbr (Fig. 2). Nonetheless, the late Maastrichtian age of micropalaeontological samples from the Dunajec, Szczepanowice and Janowice sections and the strong influence of the carbonate sedimentation may indicate the latter.

Stage 4: late Maastrichtian–Paleocene

The youngest part of the Ropianka Fm in the study area is represented by the deposits of stage S4. In the southern area, it starts with the appearance of SB4, which extends through the Korzenna, Zagórze, and Lichwin sections (Figs 12, 14). The detailed log of the Zagórze section contains the best exposed axial fragment of SB4 that marks the last major progradation of the Ropianka Fm depositional system in the study area (Fig. 12). SB4 shows internal asymmetry for a distance of ~4 km, with thinning of the sandstone beds and the entire succession from the Zagórze section toward the W (Korzenna section) and a comparable thickness and facies composition of the succession to the E (Lichwin section; Figs 12, 14). Coarse-grained and thick-bedded sandstones and conglomerates were formed in the proximal zone of the channel-lobe complex, supplied from the southern source (Węglówka Ridge), the activity of which reached its maximum during the formation of the entire sedimentary succession analysed. These deposits (~80 m thick) of the channel-fill and channel-lobe transition zone (FA3) and the lobe-axis (FA4) contain exotic material, both as scattered coarse grains in the turbidites and the deposits of concentrated flows (F1, F2), and as granules and pebble-sized components of the pebbly mudstone (F11) and muddy sandstone deposits (F4). SB4 contains the coarsest-grained material and the highest contribution of mass-movement deposits in the study area (Fig. 12). Up the Zagórze section, deposits become finer and thinner and represent mostly lobe-off-axis (FA5) and lobe-fringe (FA6) settings, still with the influence of the exotic-bearing mass-transport deposits and the increased occurrence of the marlstone (Figs 12). The top of the section is formed again by thick-bedded sandstones of the lobe-axis setting (FA4; Fig. 21). The very top of the Ropianka Fm is capped by variegated shales, at least several metres thick, of the Variegated Shale Fm (Paleocene–Eocene), which crops out in the Korzenna section, a lateral equivalent of the Zagórze section (Figs 12, 15). However, the uppermost part of the Ropianka Fm and its direct transition into the Variegated Shale Fm is not exposed.

Deposits of stage S4 are also present in the northern area. In the Dunajec-Dąbrówka Szczepanowska area, deposits of SB4 occur above the marly interval of stage S3, representing another major phase of progradation and the activity of the full spectrum of sedimentary sub-environments of the depositional lobe with a centre of sediment distribution closer to the Dunajec section (Figs 14, 16). The Dunajec and Dąbrówka Szczepanowska sections are dominated by stacked deposits of the lobe-axis (FA4), off-axis (FA5) and lobe-fringe (FA6; Fig. 14). At least locally, sedimentation

took place below or close to the lysocline depth, which is reflected in the appearance of noncalcareous variegated mudstone, observed in the Dąbrówka Szczepanowska section (Fig. 8). The palaeotransport direction indicates transport along the basin axis (directions toward the NE, E and SE). In the upper part of the Dunajec section, the deposits are thinner-bedded, with alternations of marlstone (log interval 147–195 m in Fig 14). However, poor exposure leaves an incomplete picture of this phase. The highest part of the section is represented by mudstone of uncertain stratigraphic position, ~15 m thick, which is separated from the older Dunajec deposits in Janowice-Lichwin Syncline by a thrust (Figs 14, 15). Thick-bedded deposits of SB4 also were observed in the Marginal Antlicline, in the upper parts of the Szczepanowice, Lubinka, Pleśna and Rychwałd sections (Fig. 15). The Variegated Shale Fm is absent in the northern area, owing to tectonic reduction. Therefore, the sedimentary succession remains incomplete.

Interpretation: The Zagórze section records the last major progradational-retrogradational cycle in the Ropianka Fm in the study area with the strongest pulse of coarse-grained sedimentation (FA3, FA4) accompanied by mass-movement deposits (Fig. 16). Up the Zagórze section, lobe-off-axis (FA5) and lobe-fringe deposits (FA6), with thinning and fining trends, mark the final retrogradation of the channel-lobe complex. In comparison to the previous stages, stage S4 in the Zagórze section shows more gradual fining and thinning of the retrograding depositional system (Fig. 12). The presence of relatively widely distributed facies F11 indicates a much higher slope inclination (>2–4°) than at the northern margin, which lacks widespread slope instability during the Campanian–Maastrichtian. This is in agreement with the abundance of coarse-grained sandstone and conglomerate. Reactivation of the southern source indicates a tectonic pulse that disturbed the local equilibrium profile in the southern area. This in turn led to deep erosion of the Węglówka Ridge and remobilisation of the exotic-bearing deposits, which are present in the Zagórze section (Figs 6, 12). Most of the deposits of facies F11 rest upon the sandstone of facies F1 and F2, indicating a co-genetic origin for them ('linked debrites' *sensu* Haughton *et al.*, 2003), i.e., HEBs (cf. Haughton *et al.*, 2009), but with a significantly different composition than this type of bed in the previous stages S1b, S2 and S3. The northern area experienced similar evolution but without clear signs of mass movements and such abundance of coarse-grained deposits. The palaeotransport direction at the Dąbrówka Szczepanowska section indicates the formation of another turbidite complex, supplied from the W with a fan-shaped pattern of sediment distribution along the basin axis (Fig. 16).

The occurrence of exotic-bearing coarse-grained deposits, considered to be the Makówka Slump Debrites and the Babica Clay (Kotlarczyk, 1978, 1988a), allowed recognition of stage S4 deposits as the Leszczyny Mbr, which is also confirmed by the occurrence of the Variegated Shale Fm above (Fig. 15). In the study area, the Wola Korzeniecka Mbr (Fig. 2) is absent or not exposed. The bulk progradation of the depositional system is widely recorded in the Ropianka Fm of the entire Polish segment of the Skole Basin, as an abundant occurrence of mass-movement deposits (cf.

Burzewski, 1966; Kotlarczyk, 1978, 1988a; Łapcik *et al.*, 2016; Łapcik, 2018, 2019). However, in the eastern part of the basin, they mostly were derived from the northern margin of the basin. The direct transition from the Ropianka Fm to younger deposits is not exposed, but the retrogradational trend in the upper part of the Zagórze section and the thick mud cap in the Dunajec section most likely reflect the beginning of the transgression that culminated in the deposition of the Variegated Shale Fm basinwide (Łapcik, 2019).

Sediment sources

Consistent palaeotransport directions of the siliciclastic material from the W and NW (Fig. 16) indicate a long-lasting source, which was active throughout the entire interval studied (cf. Książkiewicz, 1962), with the exception of stage S1b. Such uniform sediment routing is probably the result of established submarine canyons or gullies, which captured siliciclastic input, derived from the shelf-edge delta or delivered by longshore currents. At the same time, a carbonate shelf environment dominated the northern and northeast margins of the study area and served as a source of redeposited carbonate material (Kędzierski and Leszczyński, 2013). Shallow-marine Late Cretaceous carbonate facies are widespread outside the Carpathians in the area to the north of the study area (e.g., Karnkowski and Ołtuszyk, 1968) and are also present in the local substratum in boreholes, e.g., Wojnicz 2 at depth ~2,500–2,535 m; Pleśna 1 at depth ~2,260–2,490 m; and Tarnów 14 at depth ~1,640–2,070 m. During all distinguished stages (S1–4), the northern area evidenced the highest impact of the carbonate source, indicating its proximity to the shallower zone of the basin (Fig. 16). However, the study area shows even more complex sediment pathways, including a southern source (Węglówka Ridge) and possibly another siliciclastic source to the NE, where deposits formed only distal facies associations in the eastern part of the study area (Rychwałd and Lichwin sections; Fig. 16). Brief field observations in the area of Tarnowiec and Zawada (~8 km to the NE of the study area) confirmed the appearance of coarse-grained sandstone to conglomeratic deposits in that area. Poor exposure leaves uncertainty about their stratigraphic position, but their lithologic composition implies an affinity of these rocks to the Leszczyny Mbr (cf. Marciniec *et al.*, 2006). Their sedimentological characteristics (predominance of thick-bedded facies F1) support a possible mid- or upper-fan origin and perhaps as another channel-lobe complex, supplied from the northern basin margin. In general, the western part of the Skole Basin evidenced complex sediment routing and supply during Campanian–Paleocene times, reflecting susceptibility to sea-level change and tectonic activity (Fig. 16).

The exotic material may occur as a sandy to gravely fraction in most of the sedimentary facies described. It might represent only a small admixture but also a volumetrically important part of the deposits, e.g., in facies F11. Exotic material is widely distributed in the Ropianka Fm (see Łapcik *et al.*, 2016, and references therein), but occurs mainly closer to the northern basin slope. Qualitative observations of the exotic lithologies shows a smaller proportion of Mesozoic limestones than in the eastern area, which

is counterintuitive with respect to the distribution of pre-Tertiary rocks in the substratum of the Carpathian Foredeep. There, in an easterly direction, the substratum contains progressively older Palaeozoic and Precambrian rocks (see Karnkowski and Ołtuszyk, 1968). In the study area, exotic grains were supplied from at least two different sources, i.e., the northern marginal area and Węglówka Ridge in the south, which shows that the substratum of each has a similar geological history.

Basin topography and asymmetry

The study area appears to represent sedimentation in a relatively narrow part of the Skole Basin and this setting may have resulted in the partial confinement of gravity flows, at least during particular stages of the basin evolution. The confinement of the gravity flows is supported by strong aggradational trends and the weak compensational stacking of depositional lobe complexes, and possible flow reflections or deflections (Fig. 16). The differences between the sedimentation in the norther and southern areas through all described stages gives a partial insight into the architecture of the western part of the Skole Basin (Fig. 16). On the basis of the distribution of facies associations and palaeotransport directions, a local depocentre was located closer to or within the southern area, where flows were propagated mostly along the basin axis and parallel to the basin margins. Notwithstanding, the significant differences in grain size and the contribution of mass-transport deposits between the northern and southern areas, especially during stage S4, clearly indicate a contrast between the local inclinations of the northern and southern slopes (Fig. 16). This characteristic facies distribution in a north-south direction reveals asymmetry of the basin floor inclination and the potential location of the depocentre, which remained relatively static throughout the sedimentary history of the Ropianka Fm. However, in comparison with well-established examples of asymmetrical confined basins (cf. Tinterri and Tagliaferri, 2015; Tinterri *et al.*, 2016, 2017; Cunha *et al.*, 2017; Tinterri and Civa, 2021), this local asymmetrical facies distribution is less pronounced, perhaps owing to the mixed sand-mud character of the Skole Basin, higher efficiency of the flows, and the connection with the eastern part of the basin. The asymmetrical topography may have been inherited after the rifting stage of the proto-Silesian Basin (cf. Ślączka *et al.*, 2006; Słomka *et al.*, 2006) during the formation of the basin and the development of half-grabens, which was healed only partially during the preceding stages of the starved basin (Malata and Poprawa, 2006).

During substage S1b, basin floor topography resulted in the concentration of siliciclastic sediments in the depocentre and their propagation to the north was limited, owing to the low density of the depositing turbidity currents (Fig. 16). Some of these turbidity currents may have interacted with the northern basin margin and and were deflected toward the E, resulting in a variety of palaeotransport directions in the Szczepanowice section (Figs 13, 16). Possible confinement of the small fan, developed during substage S1b, is indicated by the abrupt disappearance of SB1 to the east. Another example of the interaction between flow and basin

topography is in the deposits of stage S3 in the Dunajec section. The log contains complex beds with repetitive traction structures, which indicate changing palaeotransport directions and hence possible flow reflection and deflection.

During stages S1–4, the sedimentation of noncalcareous to calcareous mudstone, as well as varied assemblages of foraminifers and nannoplankton, imply changes in the relationship between the aggrading seafloor and the local lysocline depth. Sedimentation plausibly occurred on the lower zones of slope to base-of-slope and therefore a mid-bathyal depth is expected. The complex distribution of the noncalcareous and poorly calcareous deposits in the study area is indicative of the diverse morphology of the sea floor, despite possible changes in relative sea level and the local lysocline depth. A few horizons of variegated shales are distinguished as characteristic chronohorizons in the Ropianka Fm and are important markers for the lithostratigraphic scheme (Kotlarczyk, 1978). Basin architecture also can be inferred from the distribution of characteristic facies in particular drill cores. The Wojnicz 2 borehole, located in the western part of the study area (Fig. 1), shows a mud-dominated succession with a variegated shales interval at a depth of 610–680 m. Variegated marlstone is reported from the well Pleśna 1 (depth ~920–925 m). Unfortunately, it is impossible to correlate boreholes with outcrops; hence, they serve only as additional indicators that can be applied to this jigsaw puzzle of basin architecture. In the outcrops studied, variegated mudstone was observed within the Ropianka Fm only in the sections at Dąbrówka Szczepanowska and east of Szczepanowice, which confirms the limited distribution of this characteristic facies. It cannot be excluded that distribution of the variegated shales was controlled by the local seafloor topography, i.e., they were preserved only on local high elevations.

CONCLUSIONS

This study significantly extends qualitative and quantitative sedimentological characteristics of the Ropianka Fm turbidite system and reveals its sedimentary processes, sediment routing, architectonic elements and depositional history in the western part of the Skole Nappe. The deposits studied were subdivided into 11 facies, representing a wide spectrum of depositional processes, including siliciclastic and carbonate turbidity currents, hybrid flows, transitional flows, debris flows, and hemipelagic sedimentation. Particular facies assemblages were grouped into 7 facies associations, representing various morphodynamic architectural elements of the turbidite system, from a sediment bypass zone and channel-fill deposits to distal-lobe-fringe and interlobe areas, as well as a marlstone-dominated slope or base-of-slope setting.

Four major stages in the Campanian–Paleocene evolution of the western Skole Basin represent progradational-retrogradational cycles and corresponding shifts from carbonate- to siliciclastic-dominated sedimentation as a result of relative sea-level changes and tectonic activity. A maximum of the turbidite system progradation is recorded in tens-of-metres-thick sand bodies (SB2–4) at the start of stages S2–4. Exceptionally, SB1 was encased in the middle (S1b) of a marl-dominated succession during stage S1. A carbonate-shelf environment dominated the northern and northeasters margin of the study area and was the source of redeposited carbonate material, mostly during the final phase of sea-level rise and mainly during the sea-level highstand and early fall. The sedimentary history of the Ropianka Fm in the study area is as follows: S1) early Campanian marlstone-dominated sedimentation (western equivalent of the Kropivnik Fucoid Marl Mbr) in the lower-slope or base-of-slope settings, which correlates with a relative sea-level highstand; S2) the late Campanian major progradation of the turbidite system with siliciclastic sedimentation (Turnica Flysch Mbr) and major sediment pathways, extending along the northern basin margin; S3) Maastrichtian sedimentation with the influence of a carbonate source; and S4) mixed carbonate-siliciclastic sedimentation (Leszczyny Mbr), with exotics-bearing mass-transport deposits (Makówka Slump Debrites and Babica Clay) and a general decreasing trend of the marlstone contribution up the sections of stage S4. This is in agreement with the general lithostratigraphic evolution of the Ropianka Fm in the eastern part of the Skole Nappe.

On the local scale, the Skole Basin shows multiple features (e.g., aggradational stacking patterns of depositional lobe deposits, the distribution of facies and facies associations, the position of the local depocentre, a narrow basin setting), leading to the conclusion that sediment gravity flows were interacting with seafloor topography or even were partially confined by local basin slopes and/or tectonic heights. Furthermore, the distribution of coarse-grained facies associations and mass-wasting deposits was interpreted as reflecting asymmetry of the basin floor with a relatively steep southern slope and a gentle northern slope. This asymmetry was at least partially controlled by the compressional tectonic activity of the evolving orogen. The complex local basin morphology is in contrast to the eastern part of the basin in the Słonne and Hucisk Jawornickie area, where the formation of channel-lobe complexes was controlled by depositional-lobe compensational stacking and distributary-channel avuslsion.

Prolonged palaeotransport directions toward the SE, E and NE are interpreted as being related to submarine canyons or gullies, which captured the siliciclastic input, derived from the shelf-edge delta or delivered by longshore currents. Sediment gravity flows moved along the axis of the basin and the basin northern and southern margins of the basin. Tectonic activity was a major trigger for temporal activation of a southern source (Węglówka Ridge) during stages S1b and S4. Varying palaeotransport directions in deposits bearing exotic components provide the evidence for similarities in the geological history of the northern and southern source areas of the Skole Basin, at least in its western part.

REFERENCES

Allen, J. R. L., 1982. *Sedimentary Structures, their Character and Physical Basis. Volumes 1, 2*. Elsevier, Amsterdam, 593 pp; 663 pp.

Amy, L. A., Kneller, B. & McCaffrey, W. D., 2000. Evaluating the links between turbidite characteristics and gross system architecture: upscaling insights from the turbidite sheet-system of the Peïra Cava, SE France. *SEPM, Gulf Coast Section, 20th Annual Research Conference, Deep-Water Reservoirs of the World*, pp. 1–15.

Amy, L. A., McCaffrey, W. D. & Kneller, B., 2007. The Peïra Cava Outlier, Annot Sandstones, France. In: Nilsen, T. H., Shew, R. D., Steffens, G. S. & Studlick, J. (eds), *Atlas of Deep-Water Outcrops. AAPG, Studies in Geology*, 56: 185–187.

Arnott, R. W. C. & Hand, B. M., 1989. Bedforms, primary structures and grain fabric in the presence of suspended sediment rain. *Journal of Sedimentary Research*, 59: 1062–1069.

Arthur, M., Dean, W. & Pratt, L., 1988. Geochemical and climatic effects of increased marine organic carbon burial at the Cenomanian/Turonian boundary. *Nature*, 335: 714–717.

Baas, J. H., Best, J. L. & Peakall, J., 2011. Depositional processes, bedform development and hybrid bed formation in rapidly decelerated cohesive (mud-sand) sediment flows. *Sedimentology*, 58: 1953–1987.

Baas, J. H., Best, J. L., Peakall, J. & Wang, M., 2009. A phase diagram for turbulent, transitional, and laminar clay suspension flows. *Journal of Sedimentary Research*, 79: 162–183.

Baas, J. H., Tracey, N. D. & Peakall, J., 2021. Sole marks reveal deep-marine depositional process and environment: implications for flow transformation and hybrid-event-bed models. *Journal of Sedimentary Research*, 91: 986–1009.

Bąk, K., Bąk, M., Górny, Z. & Wolska, A., 2014. Environmental conditions in a Carpathian deep-sea basin during the period preceding Oceanic Anoxic Event 2 – a case study from the Skole Nappe. *Geologica Carpathica*, 65: 433–450.

Barwicz-Piskorz, W. & Rajchel, J., 2012. Radiolarian and agglutinated foraminiferal biostratigraphy of the Paleogene deep-water deposits on the northern margin of the Carpathian Tethys (Skole Unit). *Geological Quarterly*, 56: 1–24.

Bell, D., Stevenson, C. J., Kane, I. A., Hodgson, D. M. & Poyatos-Moré, M., 2018. Topographic controls on the development of contemporaneous but contrasting basin-floor depositional architectures. *Journal of Sedimentary Research*, 88: 1166–1189.

Bernhardt, A., Jobe, Z. R. & Lowe, D. R., 2011. Stratigraphic evolution of a submarine channel–lobe complex system in a narrow fairway within the Magallanes foreland basin, Cerro Toro Formation, southern Chile. *Marine and Petroleum Geology*, 28: 785–806.

Best, J. L. & Bridge, J. S., 1992. The morphology and dynamics of low amplitude bedwaves upon upper stage plane beds and the preservation of planar laminae. *Sedimentology*, 39: 737–752.

Boulesteix, K., Poyatos-Moré, M., Flint, S. S., Hodgson, D. M., Taylor, K. G. & Parry, G. R., 2020. Sedimentary facies and stratigraphic architecture of deep-water mudstone beyond the basin-floor fan sandstone pinchout. *Journal of Sedimentary Research*, 90: 1678–1705.

Bouma, A. H., 1962. *Sedimentology of Some Flysch Deposits: A Graphic Approach to Facies Interpretation*. Elsevier, Amsterdam, 168 pp.

Bouma, A. H., 2000. Coarse-grained and fine-grained turbidite systems as end member models: applicability and dangers. *Marine and Petroleum Geology*, 17: 137–143.

Bown, P. R. & Young, J. R., 1998. Techniques. In: Bown, P. R. (ed.), *Calcareous Nannofossil Biostratigraphy*. Kluwer Academic Publishers, Dordrecht, pp. 16–28.

Bromowicz, J., 1974. Facial variability and lithological character of Inoceramian Beds of the Skole-Nappe between Rzeszów and Przemyśl. *Prace Geologiczne*, 84: 1–83. [In Polish, with English summary.]

Brooks, H. L., Hodgson, D. M., Brunt, R. L., Peakall, J., Hofstra, M. & Flint, S. S., 2018. Deep-water channel-lobe transition zone dynamics: Processes and depositional architecture, an example from the Karoo Basin, South Africa. *GSA Bulletin*, 130: 1723–1746.

Burnett, J. A., 1998. Upper Cretaceous. In: Bown, P. R. (ed.), *Calcareous Nannofossils Biostratigraphy*. Chapman and Hall, London, pp. 132–199.

Burzewski, J., 1966. Les marnes à Baculithes sur le fond de la lithostratigraphie des à Inocérames dans les Carpathes de ski-bas. *Zeszyty Naukowe AGH, Geologia*, 7: 89–115. [In Polish, with French summary.]

Cartigny, M. J. B., Eggenhuisen, J. T., Hansen, E. W. M. & Postma, G., 2013. Concentration-dependent flow stratification in experimental high-density turbidity currents and their relevance to turbidite facies model: *Journal of Sedimentary Research*, 83: 1047–1065.

Cieszkowski, M., Kysiak, T., Szczęch, M. & Wolska, A., 2017. Geology of the Magura Nappe in the Osielec area with emphasis on an Eocene olistostrome with metabasite olistoliths (Outer Carpathians, Poland). *Annales Societatis Geologorum Poloniae*, 87: 169–182.

Covault, J. A., Sylvester, Z., Hubbard, S. M., Jobe, Z. R. & Sech, R. P., 2016. The stratigraphic record of submarine-channel evolution. *The Sedimentary Record*, 14: 4–11.

Cunha, R. S., Tinterri, R. & Muzzi Magalhaes, P., 2017. Annot Sandstone in the Peïra Cava basin: An example of an asymmetric facies distribution in a confined turbidite system (SE France). *Marine and Petroleum Geology*, 87: 60–79.

Deptuck, M. E., Piper, D. J. W., Savoye, B. & Gervais, A., 2008. Dimensions and architecture of Late Pleistocene submarine lobes off the northern margin of East Corsica. *Sedimentology*, 55: 869–898.

Dżułyński, S., 1996. Erosional and deformational structures in single sedimentary beds: a genetic commentary. *Annales Societatis Geologorum Poloniae*, 66: 101–189.

Dżułyński, S., 2001. *Atlas of Sedimentary Structures From the Polish Flysch Carpathians*. Institute of Geological Sciences, Jagiellonian University, Kraków, 132 pp.

Edwards, A. R., 1963. A preparation technique for calcareous nannoplankton. *Micropaleontology*, 9: 103–104.

Fisher, R. V., 1983. Flow transformations in sediment gravity flows. *Geology*, 11: 273–274.

Fonnesu, M., Felletti, F., Haughton, P. D. W., Patacci, M. & McCaffrey, W. D., 2018. Hybrid event bed character and distribution linked to turbidite system sub-environments: The North Apennine Gottero Sandstone (north-west Italy). *Sedimentology*, 65: 151–190.

Gągała, Ł., Vergés, J., Saura, E., Malata, T., Ringenbach, J., Werner, P. & Krzywiec, P., 2012. Architecture and orogenic evolution of the northeastern Outer Carpathians from cross-section balancing and forward modelling. *Tectonophysics*, 532–535: 223–241.

Gardner, M. H., Borer, J. M., Melick, J. J., Mavilla, N., Dechesne, M. & Wagerle, R. N., 2003. Stratigraphic process-response model for submarine channels and related features from studies of Permian Brushy Canyon outcrops, West Texas. *Marine Petroleum Geology*, 20: 757–787.

Gasiński, M. A. & Uchman, A., 2009. Latest Maastrichtian foraminiferal assemblages from the Husów region (Skole Nappe, Outer Carpathians, Poland). *Geologica Carpathica*, 60: 283–294.

Gedl, E., 1999. Lower Cretaceous palynomorphs from the Skole Nappe (Outer Carpathians, Poland). *Geologica Carpathica*, 50: 75–90.

Geroch, S., Krysowska-Iwaszkiewicz, M., Michalik, M., Prochazka, K., Radomski, A., Radwański, Z., Unrug, Z., Unrug, R. & Wieczorek, J., 1979. Sedimentation of Węgierka Marls (Late Senonian, Polish Flysch Carpathians). *Rocznik Polskiego Towarzystwa Geologicznego*, 49: 105–134. [In Polish, with English summary.]

Golonka, J., Gahagan, L., Krobicki, M., Marko, F., Oszczypko, N. & Ślączka, A., 2006. Plate-tectonic evolution and paleogeography of the Circum-Carpathian region. In: Golonka, J. & Picha, F. J. (eds), *The Carpathians and their foreland: Geology and hydrocarbon resources. AAPG Memoir*, 84: 11–46.

Golonka, J., Krobicki, M., Waśkowska-Oliwa, A., Vašiček, Z. & Skupien, P., 2008. Main paleogeographical elements of the West Outer Carpathians during Late Jurassic and Early Cretaceous times. In: Krobicki, M. (ed.), *Utwory przełomu jury i kredy w zachodnich Karpatach fliszowych polsko-czeskiego pogranicza, Jurassica VII, 27–29.09.2008 – Żywiec/Štramberk. Kwartalnik AGH. Geologia,* 34: 61–72.

Gradstein, F., Ogg, J., Schmitz, M. & Ogg, G., 2020. *The Geological Time Scale 2020*. Elsevier, Oxford, 1390 pp.

Grundvåg, S. A., Johannessen, E. P., Hansen, W. H. & Plink-Björklund, P., 2014. Depositional architecture and evolution of progradationally stacked lobe complexes in the Eocene Central Basin of Spitsbergen. *Sedimentology*, 61: 535–569.

Gucik, S., 1963. Profile of the Lower Cretaceous from Bełwin in the Przemyśl Carpathians. *Kwartalnik Geologiczny*, 7: 257–268. [In Polish, with English summary.]

Hansen, L. A. S., Hodgson, D. M., Pontén, A., Bell, D. & Flint, S., 2019. Quantification of basin-floor fan pinchouts: Examples from the Karoo Basin, South Africa. *Frontiers in Earth Science*, 7: 1–20.

Haq, B. U. 2014. Cretaceous eustasy revisited. *Global and Planetary Change*, 113: 44–58.

Haughton, P. D. W., Barker, S. P. & McCaffrey, W. D., 2003. 'Linked' debrites in sand-rich turbidite systems – origin and significance. *Sedimentology*, 50: 459–482.

Haughton, P. D. W., Davis, C., McCaffrey, W. & Barker, S. P., 2009. Hybrid sediment gravity flow deposits – classification, origin and significance. In: Amy, L. A., McCaffrey, W. B. & Talling, P. J. (eds), *Hybrid and Transitional Submarine Flows. Marine Petroleum Geology*, 26: 1900–1918.

Hiscott, R. N. & Middleton, G. V., 1980. Fabric of coarse deep-water sandstones, Tourelle Formation, Quebec, Canada. *Journal of Sedimentary Petrology*, 50: 703–722.

Hodgson, D. M., 2009. Distribution and origin of hybrid beds in sand-rich submarine fans of the Tanqua depocentre, Karoo Basin, South Africa. *Marine Petroleum Geology*, 26: 1940–1956.

Hubbard, S. M., Covault, J. A., Fildani, A. & Romans, B. R., 2014. Sediment transfer and deposition in slope channels: Deciphering the record of enigmatic deep-sea processes from outcrop. *GSA Bulletin*, 126: 857–871.

Hubbard, S. M., Jobe, Z. R., Romans, B. W., Covault, J. A., Sylvester, Z. & Fildani, A., 2020. The stratigraphic evolution of a submarine channel: linking seafloor dynamics to depositional products. *Journal of Sedimentary Research*, 90: 673–686.

Hubbard, S. M., Romans, B. W. & Graham, S. A., 2008. Deep-water foreland basin deposits of the Cerro Toro Formation, Magallanes basin, Chile: architectural elements of a sinuous basin axial channel belt. *Sedimentology*, 55: 1333–1359.

Ilstad, T., Marr, J. G., Elverhøi, A. & Harbitz, C. B., 2004. Laboratory studies of subaqueous debris flows by measurements of pore-fluid pressure and total stress. *Marine Geology*, 213: 403–414.

Janocko, M., Nemec, W., Henriksen, S. & Warchoł, M., 2013. The diversity of deep-water sinuous channel belts and slope valley-fill complexes. *Marine Petroleum Geology*, 41: 7–34.

Kane, I. A. & Ponten, A. S. M., 2012. Submarine transitional flow deposits in the Paleogene Gulf of Mexico. *Geology*, 40: 1119–1122.

Kane, I. A., Ponten, A. S. M., Vangdal, B., Eggenhuisen, J. T., Hodgson, D. M. & Spychala, Y. T., 2017. The stratigraphic record and processes of turbidity current transformation across deep-marine lobes. *Sedimentology*, 64: 1236–1273.

Karnkowski, P. & Ołtuszyk, S., 1968. *Geological Atlas of the Polish Carpathian foreland 1:500 000*. Instytut Geologiczny, Warszawa.

Kędzierski, M. & Leszczyński, S., 2013. A paleoceanographic model for the Late Campanian–Early Maastrichtian sedimentation in the Polish Carpathian Flysch basin based on nannofossils. *Marine Micropaleontology*, 102: 34–50.

Kenyon, N. H. & Millington, J., 1995. Contrasting deep-sea depositional systems in the Bering Sea, In: Pickering, K. T., Hiscott, R. N., Kenyon, N. H., Ricci Lucchi, F. & Smith, R. D. A. (eds), *Atlas of Deep Water Environments: Architectural Style in Turbidite Systems*. Chapman and Hall, London, pp. 196–202.

Kneller, B. C. & Branney, M. J., 1995. Sustained high-density turbidity currents and the deposition of thick massive sands. *Sedimentology*, 42: 607–616.

Koszarski, L., 1961. Nowe dane o rozwoju serii skolskiej na S od Tarnowa i Wojnicza. *Kwartalnik Geologiczny*, 5: 994–995. [In Polish.]

Kotlarczyk, J., 1978. Stratigraphy of the Ropianka Formation or of Inoceramian beds in the Skole Unit of the Flysch Carpathians. *Prace Geologiczne, Polska Akademia Nauk, Oddział w Krakowie, Komisja Nauk Geologicznych*, 108: 1–75. [In Polish, with English summary.]

Kotlarczyk, J., 1988a. *Przewodnik LIX Zjazdu Polskiego Towarzystwa Geologicznego w Przemyślu.* Wydawnictwa AGH. Kraków, 298 pp. [In Polish.]

Kotlarczyk, J., 1988b. Geology of the Przemyśl Carpathians – "a sketch to the portrait". *Przegląd Geologiczny*, 36: 325–333. [In Polish, with English summary.]

Kotlarczyk, J., Jerzmańska, A., Świdnicka, E. & Wiszniowska, T., 2006. A framework of ichthyofaunal ecostratigraphy of the Oligocene–Early Miocene strata of the Polish Outer Carpathian Basin. *Annales Societatis Geologorum Poloniae*, 76: 1–111.

Kowalczewska, O. & Gasiński, M. A., 2018. Late Cretaceous foraminiferids from sections in the Zabratówka area (Skole Nappe, Outer Carpathians, Poland). *Annales Societatis Geologorum Poloniae*, 88: 71–85.

Książkiewicz, M., 1962. *Geological Atlas of Poland. Stratigraphic and Facial Problems. Fasc – 13 - Cretaceous and Early Tertiary in the Polish External Carpathians, 1:600 000.* Wydawnictwa Geologiczne, Warszawa. [In Polish, with English summary.]

Łapcik, P., 2017. Facies heterogeneity of a deep-sea depositional lobe complex: case study from the Słonne section of Skole Nappe, Polish Outer Carpathians. *Annales Societatis Geologorum Poloniae*, 87: 301–324.

Łapcik, P., 2018. Sedimentary processes and architecture of Upper Cretaceous deep-sea channel deposits: a case from the Skole Nappe, Polish Outer Carpathians. *Geologica Carpathica*, 69: 71–88.

Łapcik, P., 2019. Facies anatomy of a progradational submarine channelized lobe complex: semi-quantitative analysis of the Ropianka Formation (Campanian–Paleocene) in Hucisko Jawornickie section, Skole Nappe, Polish Carpathians. *Acta Geologica Polonica*, 69: 111–141.

Łapcik, P., 2023. Transitional flow deposits on submarine lobe flank (Veřovice and Lhoty Fms, Albian – Cenomanian, Polish Outer Carpathians). *Sedimentary Geology*, 445: 106329.

Łapcik, P., Kowal-Kasprzyk, J. & Uchman, A., 2016. Deep-sea mass-flow sediments and their exotic blocks from the Ropianka Formation (Campanian–Paleocene) in the Skole Nappe: a case study of the Wola Rafałowska section (SE Poland). *Geological Quarterly*, 60: 301–316.

Leclair, S. F. & Arnott, R. W. C., 2005. Parallel lamination formed by high-density turbidity currents. *Journal of Sedimentary Research*, 75: 1–5.

Leszczyński, S., 2003. Bioturbation structures in the Holovnia Siliceous Marls (Turonian–Lower Santonian) in Rybotycze (Polish Carpathians). *Annales Societatis Geologorum Poloniae*, 73: 103–122.

Leszczyński, S., 2004. Bioturbation structures of the Kropivnik Fucoid Marls (Campanian–lower Maastrichtian) of the Huwniki — Rybotycze area (Polish Carpathians). *Geological Quarterly*, 48: 35–60.

Leszczyński, S., Malik, K. & Kędzierski, M., 1995. New data on lithofacies and stratigraphy of the siliceous and fucoid marl of the Skole Nappe (Cretaceous, Polish Carpathians). *Annales Societatis Geologorum Poloniae*, 65: 43–62. [In Polish, with English summary.]

Lowe, D. R., 1982. Sediment gravity flows, II. Depositional models with special reference to the deposits of high-density turbidity currents. *Journal of Sedimentary Petrology*, 52: 279–297.

Lowe, D. R. & Guy, M., 2000. Slurry-flow deposits in the Britannia Formation (Lower Cretaceous), North Sea: a new perspective on the turbidity current and debris flow problem. *Sedimentology*, 47: 31–70.

Lowe, D. R., Guy, M. & Palfrey, A., 2003. Facies of slurry-flow deposits, Britannia Formation (Lower Cretaceous), North Sea: implications for flow evolution and deposit geometry. *Sedimentology*, 50: 45–80.

Malata, T., 1996. Analysis of standard lithostratigraphic nomenclature and proposal of division for Skole unit in the Polish Flysch Carpathians. *Geological Quarterly*, 40: 543–554.

Malata, T. & Poprawa, P., 2006. Evolution of the Skole Subbasin. In: Oszczypko, N., Uchman, A. & Malata, E. (eds), *Palaeotectonic Evolution of the Outer Carpathian and Pieniny Klippen Belt Basins*. Instytut Nauk Geologicznych Uniwersytetu Jagiellońskiego, Kraków, pp. 101–110. [In Polish, with English abstract.]

Marciniec, P., Zimnal, Z. & Neścieruk, P., 2006. *Szczegółowa mapa geologiczna Polski w skali 1:50 000, Arkusz Wojnicz (1000)*. Państwowy Instytut Geologiczny. [In Polish.]

Marciniec, P., Zimnal, Z. & Neścieruk, P., 2014. *Objaśnienia do szczegółowej mapy geologicznej Polski 1:50 000, Arkusz Wojnicz (1000)*. Państwowy Instytut Geologiczny – Państwowy Instytut Badawczy, Warszawa, 67 pp. [In Polish.]

Marini, M., Salvatore, M., Ravnås, R. & Moscatelli, M., 2015. A comparative study of confined vs. semi-confined turbidite lobes from the Lower Messinian Laga Basin (Central Apennines, Italy): Implications for assessment of reservoir architecture. *Marine and Petroleum Geology*, 63: 142–165.

Martin, C., Young, C. A., Valluzzi, L. & Duarte, C. M., 2022. Ocean sediments as the global sink for marine micro- and mesoplastics. *Limnology and Oceanography*, 7: 235–243.

Mayall, M., Jones, E. & Casey, M., 2006. Turbidite channel reservoirs – Key elements in facies prediction and effective development. *Marine Petroleum Geology*, 23: 821–841.

Morris, S. A., Kenyon, N. H., Limonov, A. F. & Alexander, J., 1998. Downstream changes of large-scale bedforms in turbidites around the Valencia channel mouth, north-west Mediterranean: Implications for palaeoflow reconstruction. *Sedimentology*, 45: 365–377.

Mulder, T., 2011. Gravity processes and deposits on continental slope, rise and abyssal plains. In: Hüeneke, H. & Mulder, T. (eds), *Deep-Sea Sediments. Developments in Sedimentology*, 63: 25–148.

Mutti, E., 1992. *Turbidite Sandstones*. San Donato, Milanese, Università di Parma, Agip, 275 pp.

Mutti, E., Bernoulli, D., Ricci Lucchi, F. & Tinterri, R., 2009. Turbidites and turbidity currents from Alpine 'flysch' to the exploration of continental margins. *Sedimentology*, 56: 267–318.

Mutti, E. & Normark, W. R., 1987. Comparing examples of modern and ancient turbidite systems: problems and concepts.

In: Leggett, J. K. & Zuffa, G. G. (eds), *Marine Clastic Sedimentology*. Springer, the Netherlands, pp. 1–38.

Muzzi Magalhaes, P. & Tinterri, R., 2010. Stratigraphy and depositional setting of slurry and contained (reflected) beds in the Marnoso-arenacea Formation (Langhian-Serravallian) Northern Apennines, Italy. *Sedimentology*, 57: 1685–1720.

Normark, W. R., Piper, D. J. W. & Hess, G. R., 1979. Distributary channels, sand lobes, and mesotopography of Navy submarine fan, California Borderland, with applications to ancient fan sediments. *Sedimentology*, 26: 749–774.

Oszczypko, N., 2006. Position of the Polish Outer Carpathians in the Alpine arc and their stages of development. In: Oszczypko, N., Uchman, A. & Malata, E. (eds), *Palaeotectonic Evolution of the Outer Carpathian and Pieniny Klippen Belt Basins*. Instytut Nauk Geologicznych Uniwersytetu Jagiellońskiego, Kraków, pp. 9–18. [In Polish, with English abstract.]

Owen, G., Moretti, M. & Alfaro, P., 2011. Recognising triggers for soft-sediment deformation: current understanding and future directions. *Sedimentary Geology*, 235: 133–140.

Palanques, A., Kenyon, N. H., Alonso, B. & Limonov, A. F., 1995. Erosional and depositional patterns in the Valencia channel mouth: An example of a modern channel-lobe transition zone. *Marine Geophysical Research*, 18: 103–118.

Paul, K. M., 1876. Grundzüge der Geologie der Bukowina. *Jahrbuch der Kaiserlich Königlichen Geologischen Reichs-Anstalt*, 26: 263–320.

Peakall, J., Best, J., Baas, J. H., Hodgson, D. M., Clare, M. A., Talling, P. J., Dorrel, R. M. & Lee, D. R., 2020. An integrated process-based model of flutes and tool marks in deep-water environments: Implications for palaeohydraulics, the Bouma sequence and hybrid event beds. *Sedimentology*, 67: 1601–1666.

Perch-Nielsen, K., 1985. Mesozoic calcareous nannofossils. In: Bolli, H. H., Saunders, J. B. & Perch-Nielsen, K., (eds), *Plankton Stratigraphy*. Cambridge University Press, Cambridge 1, pp. 329–426.

Pickering, K. T. & Hiscott, R. N., 2015. *Deep Marine Systems: Processes, Deposits, Environments, Tectonics and Sedimentation*. John Wiley & Sons, 672 pp.

Pickering, K. T., Hiscott, R. N., Kenyon, N. H., Ricci Lucchi, F. & Smith, R. D. A., 1995. *Atlas of Deep Water Environments: Architectural Style in Turbidite Systems*. Chapman and Hall, London, 334 pp.

Piper, D. J. W., Stow, D. A. V. & Normark, W. R., 1984. The Laurentian Fan: Sohm Abyssal Plain. *Geo-Marine Letters*, 3: 141–146.

Polish Geological Institute – National Research Institute, LiDAR data. https://baza.pgi.gov.pl/cbdg/geoportal [27.11.2023].

Polish Geological Institute – National Research Institute, boreholes data. https://otworywiertnicze.pgi.gov.pl [27.11.2023].

Prélat, A. & Hodgson, D. M., 2013. The full range of turbidite bed thickness patterns in submarine lobes: controls and implications. *Journal of the Geological Society*, 170: 209–214.

Prélat, A., Hodgson, D. M. & Flint, S. S., 2009. Evolution, architecture and hierarchy of distributary deep-water deposits: a high-resolution outcrop investigation from the Permian Karoo Basin, South Africa. *Sedimentology*, 56: 2132–2154.

Pszonka, J., Wendorff, M. & Godlewski, P., 2023. Sensitivity of marginal basins in recording global icehouse and regional tectonic controls on sedimentation. Example of the Cergowa Basin, (Oligocene) Outer Carpathians. *Sedimentary Geology*, 444: 106326.

Rajchel, J., 1990. Lithostratigraphy of the Upper Paleocene and Eocene sediments from the Skole Units. *Zeszyty Naukowe AGH, Geologia*, 48: 1–112. [In Polish, with English summary.]

Rajchel, J. & Uchman, A., 1998. Ichnological record of palaeoenvironment in the transgressive Miocene deposits of the Skole Unit in the Dubiecko region (SE Poland). *Przegląd Geologiczny*, 46: 523–529. [In Polish, with English summary.]

Reading, H. G. & Richards, M., 1994. Turbidite systems in deep-water basin margins classified by grain size and feeder system. *AAPG Bulletin*, 78: 792–822.

Schieber, J., Miclăuş, C., Seserman, A., Liu, B. & Teng, J., 2019. When a mudstone was actually a "sand": Results of a sedimentological investigation of the bituminous marl formation (Oligocene), Eastern Carpathians of Romania. *Sedimentary Geology*, 384: 12–28.

Schieber, J., Southard, J. B. & Schimmelmann, A., 2010. Lenticular shale fabrics resulting from intermittent erosion of water-rich muds – interpreting the rock record in the light of recent flume experiments. *Journal of Sedimentary Research,* 80: 119–128.

Shanmugam, G. & Moiola, R., 1995. Reinterpretation of depositional processes in a classic flysch sequence (Pennsylvanian Jackfork Group), Ouachita Mountains, Arkansas and Oklahoma. *AAPG Bulletin*, 79: 672–695.

Ślączka, A. & Kaminski, M. A., 1998. *A guidebook to excursions in the Polish Flysch Carpathians. Grzybowski Foundation Special Publication*, 6: 1–171.

Ślączka, A., Kruglow, S., Golonka, J., Oszczypko, N. & Popadyuk, I., 2006. The general geology of the Outer Carpathians, Poland, Slovakia, and Ukraine. In: Golonka, J. & Picha, F. (eds), *The Carpathians and their Foreland: Geology and Hydrocarbon Resources. AAPG Memoir*, 84: 221–258.

Ślączka, A., Renda, P., Cieszkowski, M., Golonka, J. & Nigro, F., 2012. Sedimentary basin evolution and olistolith formation: The case of Carpathian and Sicilian region. *Tectonophysics*, 568–569: 306–319.

Słomka, T., Malata, T., Leśniak, T., Oszczypko, N. & Poprawa, P., 2006. Evolution of the Silesian and Subsilesian Basins. In: Oszczypko, N., Uchman, A. & Malata, E. (eds), *Palaeotectonic Evolution of the Outer Carpathian and Pieniny Klippen Belt Basins*. Instytut Nauk Geologicznych Uniwersytetu Jagiellońskiego, Kraków, pp. 111–131. [In Polish, with English abstract.]

Southard, J. B., 1991. Experimental determination of bedform stability. *Annual Review of Earth and Planetary Sciences*, 19: 423–455.

Spychala, Y. T., Hodgson, D. M., Prélat, A., Kane, I. A., Flint, S. S. & Mountney, N., 2017. Frontal and lateral submarine lobe fringes: comparing sedimentary facies, architecture and flow processes. *Journal of Sedimentary Research*, 87: 75–96.

Stevenson, C. J., Jackson, C. A. L., Hodgson, D. M., Hubbard, S. M. & Eggenhuisen, J., 2015. Sediment bypass in deep-water systems. *Journal of Sedimentary Research*, 85: 1058–1081.

Stevenson, C. J., Peakall, J., Hodgson, D. M., Bell, D. & Privat, A., 2020. T_B or not T_B: Banding in turbidite sandstones. *Journal of Sedimentary Research*, 90: 821–842.

Stevenson, C. J., Talling, P. J., Masson, D. G., Sumner, E. J., Frenz, M. & Wynn, R. B., 2014. The spatial and temporal

distribution of grain-size breaks in turbidites. *Sedimentology*, 61: 1120–1156.

Stow, D. A. V. & Bowen, A. J., 1978. Origin of lamination in deep sea, fine-grained sediments. *Nature*, 274: 324–328.

Stow, D. A. V. & Bowen, A. J., 1980. A physical model for the transport and sorting of fine-grained sediment by turbidity currents. *Sedimentology*, 27: 31–46.

Stow, D. A. & Johansson, M., 2000. Deep-water massive sands: Nature, origin and hydrocarbon implications. *Marine Petroleum Geology*, 17: 145–174.

Strzeboński, P., 2015. Late Cretaceous–Early Paleogene sandy-to-gravelly debris flows and their sediments in the Silesian Basin of the Alpine Tethys (Western Outer Carpathians, Istebna Formation). *Geological Quarterly*, 59: 195–214.

Strzeboński, P., 2022. Contrasting styles of siliciclastic flysch sedimentation in the Upper Cretaceous of the Silesian Unit, Outer Western Carpathians: sedimentology and genetic implications. *Annales Societatis Geologorum Poloniae*, 92: 1–22.

Strzeboński, P., Kowal-Kasprzyk, J. & Olszewska, B., 2017. Exotic clasts, debris flow deposits and their significance for reconstruction of the Istebna Formation (Late Cretaceous–Paleocene, Silesian Basin, Outer Carpathians). *Geologica Carpathica*, 68: 562–582.

Sumner, E. J., Amy, L. A. & Talling, P. J., 2008. Deposit structure and processes of sand deposition from a decelerating sediment suspension. *Journal of Sedimentary Research*, 78: 529–547.

Sumner, E. J., Talling, P. J. & Amy, L. A., 2009. Deposits of flows transitional between turbidity current and debris flow. *Geology*, 37: 991–994.

Talling, P. J., 2013. Hybrid submarine flows comprising turbidity current and cohesive debris flow: deposits, theoretical and experimental analyses, and generalized models. *Geosphere*, 9: 460–488.

Talling, P. J., Masson, D. G., Sumner, E. J. & Malgesini, G., 2012. Subaqueous sediment density flows: Depositional processes and deposit types. *Sedimentology*, 59: 1937–2003.

Tinterri, R. & Civa, A., 2021. Laterally accreted deposits in low efficiency turbidites associated with a structurally-induced topography (Oligocene Molare Group. Tertiary Piedmont Basin, NW Italy). *Journal of Sedimentry Research*, 91: 751–772.

Tinterri, R., Civa, A., Laporta, M. & Piazza, A., 2020. Turbidites and turbidity currents. In: Scarselli, N., Jürgen, A., Roberts, D. G., Chiarella, D. & Bally, A. W. (eds), *Regional Geology and Tectonics, 2nd Ed., Vol. 1: Principles of Geologic Analysis*. Elsevier, pp. 441–479.

Tinterri, R., Laporta, M. & Ogata, K., 2017. Cross-currents turbidite facies tract in a structurally-confined, asymmetrical mini-basin (Priabonian-Rupelian, Ranzano Sandstone, northern Apennines, Italy). *Sedimentary Geology*, 352: 63–87.

Tinterri, R., Mazza, T. & Muzzi Magalhaes, P., 2022. Contained-reflected megaturbidites of the Marnoso-arenacea Formation (Contessa key bed) and helminthoid flysches (northern Apennines, Italy) and Hecho Group (south-western Pyrenees). *Frontiers in Earth Sciences*, 10: 817012.

Tinterri, R., Muzzi Magalhaes, P., Tagliaferri, A. & Cunha, R. S., 2016. Convolute laminations and load structures in turbidites as indicators of flow reflections and decelerations against bounding slopes. Examples from the Marnoso-arenacea Formation (northern Italy) and Annot Sandstones (south eastern France). *Sedimentary Geology*, 344: 382–407.

Tinterri, R. & Tagliaferri, A., 2015. The syntectonic evolution of foredeep turbidites related to basin segmentation: Facies response to the increase in tectonic confinement (Marnoso-arenacea Formation, Miocene, Northern Apennines, Italy). *Marine and Petroleum Geology*, 67: 81–110.

Uhlig, V., 1888. Ergebnisse geologischer Aufnahmen in den west-galizischen Karpathen. I. Theil. Die Sandsteizone zwischen dem penninischen Klippenzuge und dem Nordrande. *Jahrbuch der Kaiserlich-Königlichen Geologischen. Reichsanstalt*, 38: 83–264.

van Hinsbergen, D. J. J., Torsvik, T. H., Schmid, S. M., Maţenco, L. C., Maffione, M., Vissers, R. L. M., Gürer, D. & Spakman, W., 2020. Orogenic architecture of the Mediterranean region and kinematic reconstruction of its tectonic evolution since the Triassic. *Gondwana Research*, 81: 79–229.

Waśkowska, A., Joniec, A., Kotlarczyk, J. & Siwek, P., 2019. The Late Cretaceous Fucoid Marl of the Ropianka Formation in the Kąkolówka Structure (Skole Nappe, Outer Carpathians, Poland) – lithology and foraminiferal biostratigraphy. *Annales Societatis Geologorum Poloniae*, 89: 259–284.

Wynn, R. B., Kenyon, N. H., Masson, D. G., Stow, D. A. & Weaver, P. P., 2002. Characterization and recognition of deep-water channel-lobe transition zones: *AAPG Bulletin*, 86: 1441–1446.

Young, J. R., Bown, P. R. & Lees, J. A., 2022. *Nannotax3 website*. International Nannoplankton Association. www.mikrotax.org/Nannotax3 [27.11.2023.]

Żytko, K., Gucik, S., Ryłko, W., Oszczypko, N., Zając, R., Garlicka, I., Nemčok, J., Eliáš, M., Menčík, E., Dvořák, J., Straník, Z., Rakús, M. & Matejovska, O., 1989. *Geological map of the Western Outer Carpathians and their foreland without Quaternary formations*. In: Poprawa, D. & Nemčok, J. (eds), *Geological Atlas of the Western Outer Carpathians*. Polish Geological Institute.